*The Company of* **Biologists**

# RESEARCH ARTICLE

# Δ133p53 coordinates ECM-driven morphogenesis and gene expression in three-dimensional mammary epithelial acini

Sun-Young Lee[1,*,‡], Claire Robertson[1,2], Alexandra Diot[3], Valerie Meuray[3], Jean-Christophe Bourdon[3] and Mina J. Bissell[1,‡]

## ABSTRACT

Growing evidence indicates that p53 (encoded by *TP53*) has a crucial role in normal tissue development. The role of the canonical p53 (p53α) and its 12 isoforms in development and homeostasis of healthy tissue remains poorly understood. Here, we demonstrate that the Δ133p53 isoforms, the three short isoforms of p53, respond specifically to laminin-111 and play an important regulatory role in formation of mammary organoids in concert with p53α. We demonstrate that down-modulation of Δ133p53 isoforms leads to changes in gene expression of the extracellular matrix molecules fibronectin (FN), EDA⁺-FN, laminin α5 and laminin α3 in human breast epithelial cells. These changes resulted in increased actin stress fibers and enhanced migratory behavior of cells in two-dimensional culture. We found that α5β1-integrin coupled with the extracellularly deposited EDA⁺-FN activates the Akt signaling pathway in three-dimensional (3D) culture when Δ133p53 is dysregulated. Cells that do not express detectable Δ133p53 isoforms or express low levels of these isoforms failed to form polarized structures in 3D. These results uncover that Δ133p53 isoforms coordinate expression and deposition of organ-specific ECM molecules that are critical for maintenance of tissue architecture and function.

KEY WORDS: Δ133p53, ECM, Fibronectin, Laminin, Mammary epithelial cells, p53, 3D culture, Tissue polarity, Tissue architecture

## INTRODUCTION

In glandular tissues, epithelial cells constantly sense biochemical and biomechanical cues from their surrounding microenvironment, coordinate signaling events, and regulate gene expression patterns required for tissue specificity and homeostasis (Bissell et al., 2002, 1999; Nelson and Bissell, 2006). Interaction between mammary epithelial cells and the extracellular matrix (ECM), a crucial component of the microenvironment, is a central mechanism determining mammary tissue-specific structure and function (Streuli et al., 1991). In particular, laminin-111 (Ln-1; comprising α1, β1 and γ1 subunits, encoded by *LAMA1*, *LAMB1* and *LAMC1*),

one of the major constituents of the ECM, activates signaling pathways that are necessary for differentiation and polarization of breast epithelial cells (Furuta et al., 2018; Streuli et al., 1995). Two other key components of the ECM, fibronectin and type I collagen, support cell adhesion, migration, and proliferation (Egeblad et al., 2010; Pankov and Yamada, 2002), and have been shown to be required for lobuloalveolar differentiation (Liu et al., 2010) and branching morphogenesis (Berdichevsky et al., 1994; Sakai et al., 2003).

As the ECM is an essential regulator of cellular behavior and morphogenesis, its production, deposition and degradation are tightly controlled during organ development. Deregulated ECM processes might lead to changes in tissue architecture and integrity (Lu et al., 2011). Accordingly, many studies have focused on understanding how the local ECM microenvironment regulates cellular behavior, what signal pathways are involved in ECM-directed formation of organoids and what regulatory mechanisms influence tissue-specific gene expression (Alcaraz et al., 2008; Barcellos-Hoff et al., 1989; Fiore et al., 2017; Petersen et al., 1992; Xu et al., 2007). Consequently, our studies and those of other researchers demonstrate that p53 is one of the critical mediators of Ln-1-directed normal mammary morphogenesis (Furuta et al., 2018), and that mutant p53 disrupts mammary acinar morphogenesis (Freed-Pastor et al., 2012; Zhang et al., 2011).

It is well documented that p53 is mutated in most cancers including breast cancer (Hollstein et al., 1991). Despite the vast literature on p53 and its wide array of functions, little is known about the role of p53 in normal mammary gland development. However, emerging evidence showing that p53 plays a regulatory role in development highlights the importance of p53 in mammary gland differentiation and development. Human mammary epithelial cells expressing p53 undergo growth arrest and form polarized acinus-like structures in Ln-1-rich ECM gels (lrECM), whereas cells with suppressed p53 expression form disorganized aggregates (Seewaldt et al., 2001). Moreover, heterozygous p53 deletion in mice results in delayed and disorganized mammary gland ductal morphogenesis (Gatza et al., 2008).

Understanding this crucial role of p53 in normal mammary gland-specific development and function is complicated by the existence of 12 different isoforms of p53 (Fig. 1A), which contributes to the intricate complexity of the p53 regulatory network (Flaman et al., 1996; Khoury and Bourdon, 2011). A number of studies have shown that different p53 isoforms have distinct functions and can modulate activity of the canonical p53 (p53α) (Bourdon et al., 2005; Fujita et al., 2009), resulting in pathological outcomes (Avery-Kiejda et al., 2014; Bernard et al., 2013). However, an important limitation of previous studies is that these were all performed in two-dimensional (2D) plastic dishes where all cells lose their tissue-specific architecture and function, and thus do not recapitulate *in vivo* context (Bissell, 1981). It is therefore

[1]Biological Systems and Engineering Division, Lawrence Berkeley National Laboratory, Berkeley, CA 94720, USA. [2]Material Engineering Division, Lawrence Livermore National Laboratory, Livermore, CA 94550, USA. [3]Jacqui Wood Cancer Centre, School of Medicine, University of Dundee, Dundee DD1 9SY, UK.
*Present address: Korea Nanobiotechnology Center, Pusan National University, Busan 46241, Republic of Korea.

‡Authors for correspondence (symoonlee@lbl.gov; symoonlee@pusan.ac.kr; mjbissell@lbl.gov)

S.-Y.L., 0000-0003-4970-241X; C.R., 0000-0002-3059-5135; V.M., 0000-0001-9850-1935; J.-C.B., 0000-0003-4623-9386; M.J.B., 0000-0001-5841-4423
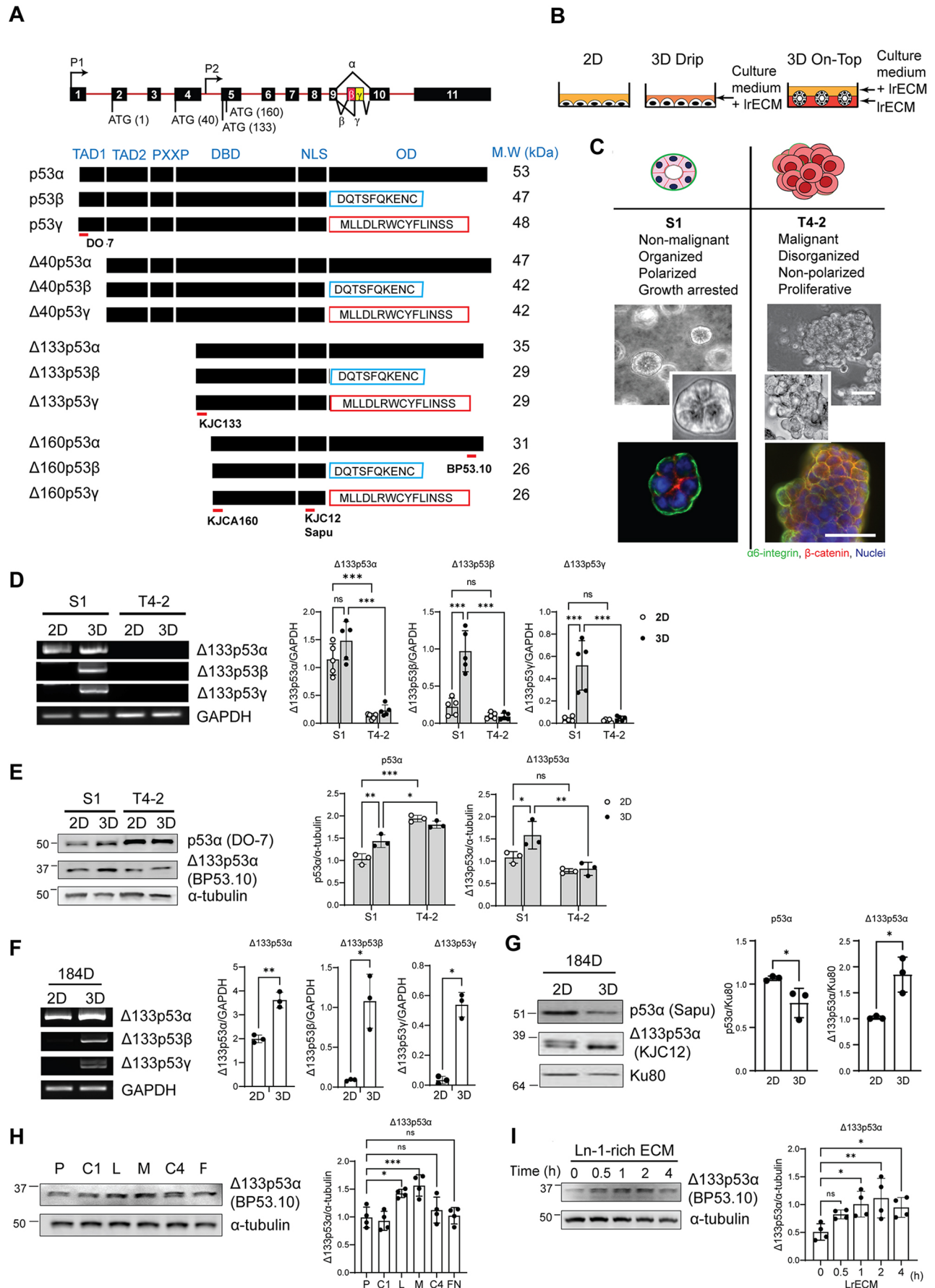
**Fig. 1.** See next page for legend.

**Fig. 1. p53 isoforms are differentially expressed in HMT-3522 human breast epithelial cells, and the expression of Δ133p53 is increased by lrECM.** (A) The human p53 gene comprises 11 exons and 10 introns, and the p53 protein has six proposed domains: the two transactivation domains (TAD1 and TAD2), the proline-rich PXXP motif, the DNA-binding domain (DBD), the nuclear localization signal (NLS) domain, and the oligomerization domain (OD). The 12 different isoforms are produced from the p53 gene. p53α is generated by splicing of the entire exons. p53β and p53γ isoforms are generated by splicing of exons 1–9, and alternative splicing of intron 9. Δ40p53, Δ133p53 and Δ160p53 isoforms are generated by alternative translation or alternative transcriptional initiation at an internal promoter. These isoforms form three distinct C-termini by alternative splicing of intron 9 (α, β and γ). The red bars indicate the regions recognized by the antibodies used in this study. (B) Scheme illustrating 2D and 3D (Drip and On-top) culture. In 2D culture, cells are plated on a tissue culture plastic surface. 3D-Drip culture is an alternative method of 3D On-top culture suitable for analysis of gene expression changes upon ECM signaling. In 3D On-top culture, cells are plated on top of a thin lrECM layer suitable for morphometric analysis as well as assessment of gene expression changes upon ECM signaling. (C) Schematic representation of morphological characteristics of HMT-3522 progression series in 3D culture (top). Bright-field microscope images of non-malignant S1 and malignant T4-2 cells in 3D On-top culture (middle) and immunostaining (bottom) for α6-integrin (green) basal and β-catenin (red) basolateral polarity markers. Nuclei are counterstained with DAPI (blue). Images representative of multiple numerous introductory experiments. Scale bars: 20 μm. (D) Representative nested RT-PCR result and densitometric analysis of the PCR data. *N*=5. RNA expression of endogenous Δ133p53 isoforms was measured in S1 and T4-2 cells in 2D or 3D lrECM culture. The cells were treated with lrECM for 4 h in 3D-Drip culture. GAPDH was used as an internal control. (E) Immunoblot analysis of endogenous p53α and Δ133p53α isoforms in S1 and T4-2 cells grown in 2D or 3D On-Top culture. α-tubulin was used for a loading control. The blots are representative of three independent experiments. Antibody used for immunoblotting analysis is indicated in parentheses. (F) Representative nested RT-PCR of endogenous Δ133p53 isoforms in 184D cells in 2D or 3D and densitometric analysis of the PCR data. *N*=3. The cells were treated with lrECM for 4 h in 3D-Drip culture. GAPDH was used as an internal control. (G) Immunoblot analysis of endogenous p53 isoforms in finite HMEC 184D cells grown in 2D or 3D lrECM. Ku80 was used for a loading control. The blots are representative of three independent experiments. (H) Representative immunoblot for Δ133p53α in S1 cells grown in different ECM proteins. P, plastic; C1, type1 collagen; L, laminin-111; M, Matrigel®; C4, type IV collagen; F, fibronectin. *N*=4. (I) Expression of endogenous Δ133p53α protein was measured as a function of time in response to lrECM in S1 cells. The blots are representative of four independent experiments. All quantitative results show mean±s.e.m. *P<0.05; **P<0.01; ***P<0.001; n.s., not significant [two-way ANOVA followed by Bonferroni's post-hoc test for multiple comparison (D,E), two-tailed unpaired *t*-test in (F,G), or one-way ANOVA followed by Dunnett's post-hoc test in (H,I)].

important to investigate the functions of p53 and its isoforms in a physiologically relevant context.

Given the reported link between Ln-1 and p53 signaling necessary for normal tissue development and function (Furuta et al., 2018), we asked whether p53 isoforms are also involved in regulation of mammary gland morphogenesis in the three-dimensional (3D) microenvironment. We found that among the 12 isoforms, the three Δ133p53 isoforms play crucial role in regulating ECM production that is essential for normal tissue development and function by coordinating the activity of p53α.

## RESULTS

### Expression of Δ133p53 is correlated with formation of polarized acinar structures

To identify the p53 isoforms that are involved in mammary gland morphogenesis, we first surveyed the expression of p53 isoforms in the unique human breast cancer progression series (HMT-3522), consisting of non-malignant (S1) and malignant (T4-2) cell lines

(Briand et al., 1996, 1987), in both 2D and 3D (Fig. 1B,C; Fig. S1A, C,D). Nested PCR of the overall mRNA expression of Δ133p53 subclasses (Δ133p53α, Δ133p53β and Δ133p53γ) showed that all three isoforms are expressed at higher levels in S1 compared to T4-2 cells, in both 2D and 3D culture (Fig. 1D). Δ133p53β and Δ133p53γ appear to be less abundant than Δ133p53α, but both are significantly upregulated in S1 cells in 3D culture in lrECM. To identify p53 isoform proteins, we used a panel of antibodies that recognize different epitopes (Fig. 1A); DO-7 was used to detect full-length p53 isoforms (p53α, p53β and p53γ) as the antibody epitope is located within TAD1 domain. BP53.10 detects α subclasses of all isoforms. Sapu and KJC12 detect all isoforms, but Sapu has a higher affinity for full-length p53 (p53α, p53β and p53γ) and Δ40p53 (Δ40p53α, Δ40p53β and Δ40p53γ) than Δ133p53 and Δ160p53 isoforms (Khoury and Bourdon, 2010). KJC133 specifically recognizes Δ133p53 isoforms, and KJCA160 recognizes Δ160p53 isoforms. Immunoblotting analysis confirmed that Δ133p53α is the form predominantly expressed in HMT-3522 cells (Fig. S1A), and its level was higher in S1 than in T4-2 cells. However, we found no significant difference in expression of Δ160p53 and Δ40p53 isoforms (Fig. S1A,C). BP 35.10 antibody consistently showed that the Δ133p53α isoform exhibited an increased expression in S1 compared to T4-2 cells in 3D culture (Fig. 1E). Taken together, we conclude that Δ133p53 isoforms are the major isoforms that are differentially expressed in S1 cells in response to Ln-1 signaling. To ascertain that this finding is not restricted only to HMT-3522 cells, we also tested non-malignant finite lifespan 184D human breast cells (Stampfer and Bartley, 1985), where we observed a similar upregulation of Δ133p53 isoforms in response to lrECM in 3D culture compared to in non-malignant S1 cells at both protein and RNA levels in 3D culture (Fig. 1F,G). Of note, we observed two distinct protein bands around the predicted molecular mass of Δ133p53α in the 184D 2D sample (Fig. 1G). Given that the KJC12 antibody that we used for the immunoblotting recognizes all isoforms, there is a possibility that these cells could also be expressing the Δ160p53α isoform.

To determine whether increased Δ133p53 expression in S1 cells is regulated by cell–ECM interactions, we measured Δ133p53α levels after addition of an overlay of Ln-1 (drip culture). S1 cells showed increased expression of the isoform following Ln-1 exposure (Fig. 1H,I). Moreover, the expression of Δ133p53α was observed at 30 min after lrECM treatment, and this progressively increased and peaked at 2 h, and declined thereafter. These data indicate that Ln-1 induced upregulation of Δ133p53α expression and might modulate the cellular concentration of the isoform in a controlled manner in human breast epithelial cells.

We had shown previously that down-modulation of individual signaling pathways in malignant tumor cells (T4-2) cultured in 3D re-establishes a 'normal' phenotype (hereafter called reverted cells) that resembles their non-malignant counterpart cells (S1) (Fig. S1B) (Wang et al., 1998; Weaver et al., 1997). Upon reverting T4-2 cells with AIIB2 (an β1-integrin function blocking antibody) or PD98059 (MAPK inhibitor) in 3D lrECM, we found that protein expression of p53α and Δ133p53α were upregulated in reverted T4-2 cells to levels comparable to in S1 cells (Fig. S1C). To assess expression pattern of p53 isoforms in the context of acinar phenotype, we compared the mRNA expression of p53 isoforms in reverted T4-2 cells grown in 3D on-Top culture to S1 and T4-2 cell grown in 2D and 3D (On-Top) culture using quantitative real-time RT-PCR (qPCR) (Fig. S1D). Given that the amplicon sizes of individual p53 isoforms, ranging from 700 to 1200 base pairs in length, are not optimal for qPCR, each subclass of p53 isoforms

(i.e. α, β and γ subclasses), was collectively amplified. qPCR data showed that all the subclasses are expressed at higher levels in S1 and reverted T4-2 cells that form organized acinar structures than in those grown in 2D or in disorganized T4-2 cells (Fig. S1D). In addition, mRNA quantification of Δ133p53 subclasses (α and β/γ) confirmed the increased expression of Δ133p53 isoforms in S1 cells grown in 3D and reverted T4-2 cells (Fig. S1D). These results suggest that Δ133p53 isoforms might play a regulatory role in acinar morphogenesis in response to extracellular cues.

## Loss of Δ133p53 expression results in disordered cell movement in mammary epithelial cells

In order to investigate the function of Δ133p53 isoforms in normal breast epithelia, we silenced the expression of these isoforms in non-malignant S1 cells. Since the three Δ133p53 isoforms (Δ133p53α, Δ133p53β and Δ133p53γ) are generated using an alternative transcription initiation site in intron 4 of the *TP53* gene (Fig. 2A), we used two independent shRNA constructs specifically targeting the 5′UTR of Δ133p53 transcripts (shΔ133-1 and shΔ133-2). Knockdown of Δ133p53 isoforms was confirmed by nested RT-PCR (Fig. 2B). All subclasses of Δ133p53 isoforms were efficiently downregulated without changing the expression of full-length p53α. Given that Δ133p53 isoforms share a common 5′UTR region, the phenotype observed in-knockdown cells could be the result of depletion of Δ133p53α or Δ133p53β/γ, or all isoforms. Thus, in this manuscript Δ133p53 isoforms will be collectively referred to as Δ133p53.

Next, we monitored cell growth rate over a period of 10 days for both control and-knockdown cells. Growth curve analysis showed that Δ133p53 knockdown S1 cells continued to proliferate beyond confluence, whereas control S1 cells reduced proliferation as they reached near-confluent density (Fig. 2C). In contrast to the uniform morphology of the control cells, knockdown of Δ133p53 resulted in significant morphological changes. These cells displayed increased cell size, irregular colony boundaries and flattened colony shape compared to controls (Fig. 2D*a–f*). Since cell size and shape are regulated by cytoskeleton (Fletcher and Mullins, 2010), we analyzed changes in the actin cytoskeletal organization in both control and Δ133p53-knockdown cells. We found that knockdown of Δ133p53 increased actin stress fiber density and altered actin distribution within cells (Fig. 2D*g–l*). Depth-coded confocal images of phalloidin showed that in control cells, actin was principally located in cell–cell junctions at all *z*-planes (Fig. 2D*m,p,s*), whereas in Δ133p53-knockdown cells, strong actin density could be seen at the colony boundary and within cell bodies, whereas cell-cell junctions lacked actin staining (Fig. 2D*n,o,q,r,t*). Quantification of this phenotype using image analysis revealed that both actin intensity (Fig. 2E, left) and the area of the cell (Fig. 2E, right) significantly increased in the-knockdown cells compared to control. *xz* and *yx* cross-sections from confocal stacks of phalloidin-stained control and-knockdown cells also revealed that the lateral actin filaments of the epithelial layer are misaligned in the-knockdown cells compared with the control (Fig. 2F). Furthermore, colony morphology altered, in that cells piled up on top of each other in disorganized multiple layers, suggesting loss of contact inhibition and proliferation control. These data suggest that loss of Δ133p53 expression dysregulates actin organization in human mammary epithelial cells. The presence of actin stress fibers not only reflects changes in actin organization, which gives cells their specific morphology, but also implies that biochemical changes occurred in their surrounding microenvironments. Given the dysregulation of actin in-knockdown cells, these results imply that Δ133p53 is

necessary for proper cell motility in response to cellular microenvironment.

The actin cytoskeleton is responsible for a number of critical cellular processes including morphogenesis, polarization, and motility (Hall, 1998; Schöck and Perrimon, 2002). Given that we observed the reorganization of cytoskeleton in Δ133p53-knockdown cells, we investigated further the behavior of Δ133p53-knockdown cells through their migratory behavior using a wound healing assay. We found that-knockdown cells closed the gap faster, with the cell front moving at $3.94 \times 10^6$ μm²/h compared with $3.10 \times 10^6$ μm²/h in control cells (Fig. S2A,B; Movies 1 and 2). These results suggest that knockdown of Δ133p53 promotes cell migration and connects the observed actin organization defects to a change in cellular behavior. Consistent with this result, Boyden chamber assays also showed that-knockdown cells were more migratory than control cells (Fig. 2G). A higher magnification view of migrated cells through a Transwell exhibited a close contact between the cells, suggesting that groups of cells migrate collectively rather than individually (Fig. 2G, bottom). These data indicate that Δ133p53 regulates cell migratory behavior in human mammary epithelial cells through modulation of actin, which likely results in altered mammary gland morphogenesis.

## Δ133p53 regulates ECM production and deposition

We have shown previously that interactions between the microenvironment and mammary epithelial cells can regulate the expression of ECM molecules (Streuli and Bissell, 1990). This led us to hypothesize that the morphological changes and increased migratory behavior in Δ133p53-knockdown cells might be due to altered interactions between breast epithelial cells and ECM, and/or changes in ECM expression. Consistent with this hypothesis, expression of the total fibronectin (FN) was increased by >5-fold compared to the controls (Fig. 3A; Fig. S3A). It is known that fibronectin undergoes spliced variation (Jarnagin et al., 1994), and EDA⁺ variant fibronectin (EDA⁺-FN) promotes cell proliferation (Losino et al., 2013). We quantified EDA⁺-FN expression and found a 3–6-fold increase in Δ133p53-knockdown cells compared with controls (Fig. 3A; Fig. S3A). Whereas expression of laminin α3 (LAMA3) was downregulated by >2-fold, laminin α5 (LAMA5) was increased >6-fold by knockdown of Δ133p53. However, the expression of laminin α1 (LAMA1) was not affected (Fig. S3A). Similar results were obtained from Δ133p53-knockdown MCF10A cells (Fig. S3B). Furthermore, immunofluorescence detection of EDA⁺-FN showed that Δ133p53 knockdown in both S1 and MCF10A cells results in EDA-containing FN deposition that is organized into an extracellular fibrillar network (Fig. 3B, top and bottom; Fig. S4). We also observed the deposition of EDA⁺-FN around the 3D structure of Δ133p53-knockdown cells. In addition, α5-integrin, a partner of the β1-integrin, which together recognize FN, colocalized with EDA⁺-FN (Fig. 3B, middle), suggesting that extracellularly deposited FN is engaged with the α5β1-integrin. These data confirm that Δ133p53 is responsible for part of the program regulating the expression and proper deposition of ECM molecules in mammary epithelial cells.

Given that we observed an increased expression of FN in Δ133p53-knockdown cells, this could indicate that the cell surface receptors for FN, integrin α5 and β1 would also be upregulated. To test this, we measured the expression of integrin α5 and β1 by immunoblot analysis. We compared the level of the integrin with that in T4-2 cells because our previous study showed that expression of EDA+-FN and its corresponding receptor, α5β1-integrin were upregulated in malignant T4-2 cells compared to non-malignant S1
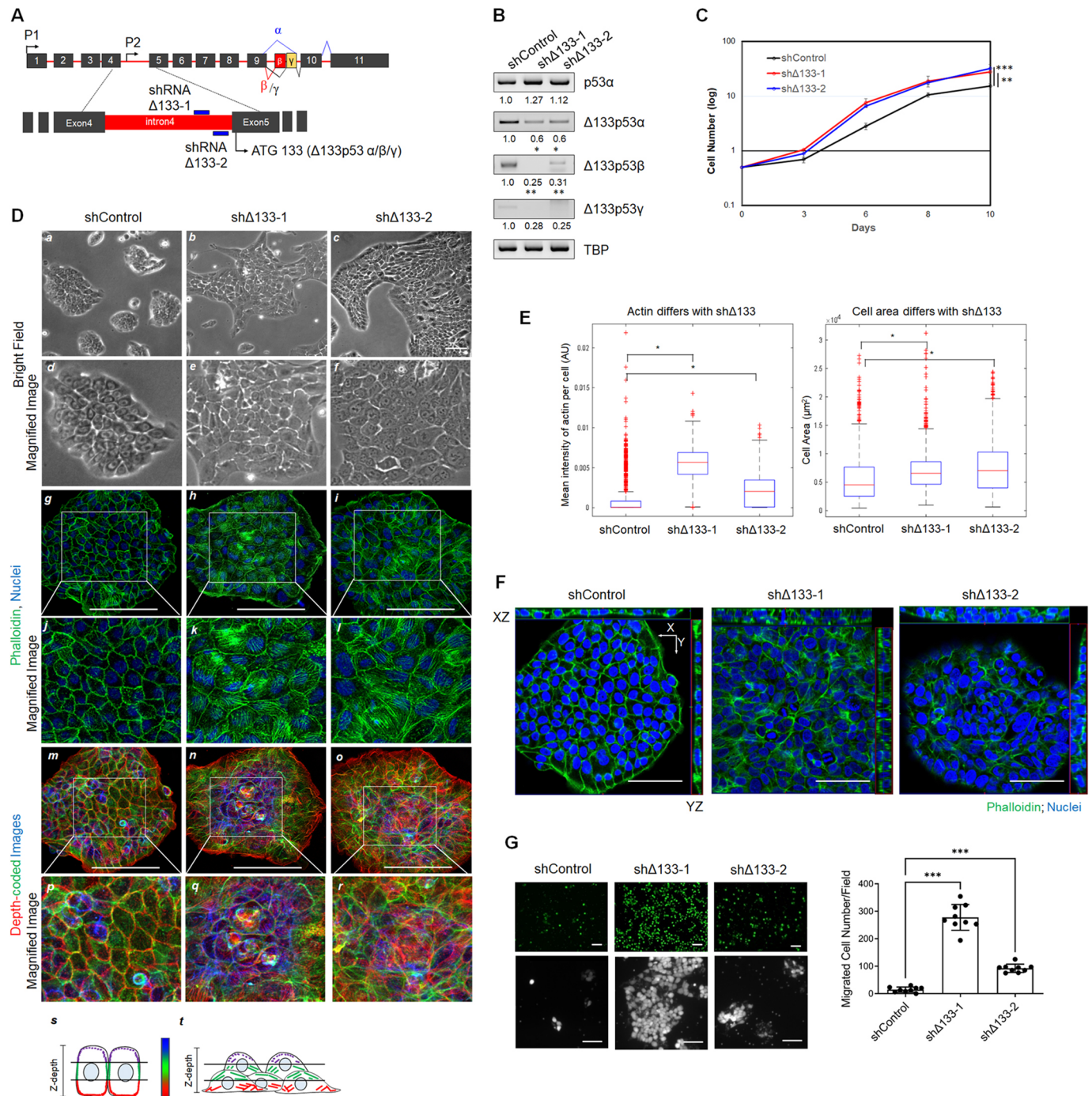
**Fig. 2.** See next page for legend.

cells (Nam et al., 2010). The results confirmed that β1-integrin and α5-integrin are upregulated in Δ133p53 knockdown S1 and MCF10A cells (Fig. 3C,D), suggesting that increased FN leads to upregulation of its cognate integrin receptors. We next asked whether α5β1-integrin-mediated recognition of the extracellularly deposited FN is responsible for driving the uncontrolled growth of Δ133p53-knockdown cells. To address this question, we inhibited the receptor activity of β1-integrin using an inhibitory monoclonal antibody (AIIB2) in 3D culture (Fig. 3E). T4-2 cells were used to validate the efficacy of AIIB2 (Weaver et al., 1997). We observed that the disorganized morphology of Δ133p53-knockdown cells was rescued by inhibition of β1-integrin,

resulting in the organized acinar phenotype, similar to what is seen in shControl and reverted T4-2 cells. Immunoblot analysis showed that inhibition of β1-integrin in Δ133p53-knockdown cells in 3D lrECM culture downregulates the activity of Akt proteins (i.e. less phosphorylated Akt relative to total Akt was found), a key downstream effector of β1-integrin/phosphoinositide 3-kinase (PI3K) signaling cascade associated with cell proliferation and survival (Fig. 3F). These data suggest that α5β1-integrin senses the disproportionately deposited FN around Δ133p53-deficient cells and subsequently activates β1-integrin-associated pathways that promote uncontrolled cell growth. Collectively, these data indicate that Δ133p53 coordinates

**Fig. 2. shRNA-mediated silencing of Δ133p53 isoforms in non-malignant S1 cells leads to cytoskeletal reorganization.** (A) Schematic diagram showing region targeted in Δ133p53 isoforms. P1 and P2 indicate promoters located in upstream of exon 1 and internal promoter located on intron 4, respectively. Two different shRNAs (shΔ133-1 and shΔ133-1) located in the 5′UTR region of Δ133p53 isoforms were used for silencing. (B) Expression of Δ133p53 isoforms in knockdown cells grown in 2D was confirmed by nested RT-PCR using primers specific for Δ133p53α (35 cycles), Δ133p53β (35 cycles), and Δ133p53γ (40 cycles). TATA-binding protein (TBP) was used for an internal control. DNA gel is displayed with inverted color. Densitometry was performed to give value for blots shown under the gel (mean of $N$=5). (C) The growth of shRNA control (shControl) and Δ133p53-knockdown cells (shΔ133-1 and shΔ133-1) in 2D was measured for 10 days. The cells were plated 20,000 cells per well. $N$=5. (D) Phase contrast morphology of the shControl or Δ133p53-knockdown cells grown on a monolayer (a–f). Confocal images of actin cytoskeleton detected with fluorescein Phalloidin (green) (g–i) and enlarged images of white boxes in d–f (j–l). Nuclei were counterstained with DAPI (blue). Monochromatic z-slices of d, e and f were colored with three different colors (6 slices from the apex with purple, 6 slices of the middle with green, and 6 slices from the bottom with red), and the images were stacked. Each color represents actin filaments at three different depths (m–o) and enlarged images of white boxes in m–o (p–r). Schematic underneath shows the alignment of actin fibers in shControl (s) and Δ133p53-knockdown cells (t). Corresponding z-depths encoded with each color are indicated with black lines. Scale bars: 100 μm. $N$=3. (E) Quantification of intensity of actin (left) and area of cells (right) by analyzing using Cellprofiler ($n$=5000 cells). The box represents the 25–75th percentiles, and the median is indicated. The whiskers show the 90th–10th percentile limits, and outliers (+) are plotted in red. (F) Representative confocal microscope images of filamentous actin (F-actin) stained with fluorescein Phalloidin (green). Nuclei were counterstained with DAPI. xz and yz cross-sections of images are shown for visualization of transverse pattern of actin filaments. Scale bars: 100 μm. $N$=3. (G) Representative micrograph of migrated control or Δ133p53-knockdown cells. Cells that migrated through a Transwell were visualized by staining with Calcein AM (left) and quantified (right). A higher magnification view of migrated cells is also shown (bottom row of images). The migrated cells were counted in five randomly chosen fields. Data are representative of triplicates in three independent experiments. Scale bars: 100 μm. All quantitative results show mean±s.e.m. *$P$<0.05; **$P$<0.01; ***$P$<0.001 [two-way ANOVA followed by Bonferroni's post-hoc test for multiple comparison (C), one-way ANOVA with Dunnett's post-hoc test for multiple comparison (B,E,G)].

morphogenesis by regulating expression and deposition of ECM components in mammary epithelial cells.

### Δ133p53 regulates the expression of fibronectin in concert with p53α

Given that depletion of Δ133p53 increases transcripts of fibronectin substantially (Fig. 3A; Fig. S3A), we assessed whether Δ133p53 is directly involved in transcriptional regulation of fibronectin. To this end, we generated a luciferase reporter connected to the fibronectin promoter, which contains a cAMP-responsive element (CRE), a CAAT box, an SP-1 motif, an AP-2 motif and a TATA box (Bernath et al., 1990) (Fig. S3C). The fibronectin promoter-driven luciferase activity was decreased by overexpression of p53α in a dose-dependent manner (Fig. S3D), and co-expression with Δ133p53 isoforms further repressed the activity by ∼2-fold (Fig. 4A). These data provide a molecular basis for the altered cell morphology and migratory behavior observed in our previous experiments (Fig. 2D, G; Fig. S2A,B; Movies 1 and 2).

Given that we observed the transcriptional repression of FN promoter activity by co-expression of p53α with Δ133p53, this raises a possibility that the repression might be achieved through an interaction between p53α and Δ133p53. Indeed, the physical interactions of Δ133p53 with p53α was confirmed by co-immunoprecipitation (Fig. 4B), suggesting that Δ133p53

regulates expression of fibronectin in company with p53α. Furthermore, we observed that the molecular mass of p53 was altered by knockdown of Δ133p53 (Fig. 4C,D; Fig. S3E). A survey of phosphorylation of p53 in both S1 and MCF10A cells revealed that knockdown of Δ133p53 induces phosphorylation on serine 392 of p53α (Fig. 4C,D). These results further indicate the interaction of Δ133p53 with p53α.

### Δ133p53 is required for establishing and maintaining a polar acinar structure

In 3D lrECM, non-malignant breast epithelial cells form highly organized structures reminiscent of the normal acinar structure in human breast, and undergo growth arrest (Briand et al., 1987; Petersen et al., 1992). Our previous study using 3D lrECM cultures demonstrated that single cells undergo multiple rotations as they divide and organize into acini. This is referred to as 'coherent angular motion' (CAMo) (Tanner et al., 2012) and it is crucial for establishment and maintenance of breast tissue polarity. In addition, that study showed that cortical actin filament was polarized in S1 cells, whereas it became randomly distributed in T4-2 cells after an initial cellular rotation, suggesting a possible association between actin organization and CAMo. Given our results that downregulating the expression of Δ133p53 impacts actin organization and cell motility, we assessed whether knockdown of the isoform impairs this coherent rotation. When control cells (shControl) were plated in 3D lrECM, they showed tight cell-cell adhesion, and underwent coherent rotation in acinar formation (Fig. 5A, top; Movie 3). However, Δ133p53-knockdown cells did not display the CAMo (Fig. 5A, bottom; Movie 4), and they were unable to organize into acinar structures. In addition, control cells fluorescently labelled with the lipophilic tracer DiI showed polarized distribution of organelles, whereas in knockdown cells organelles were distributed randomly (Fig. 5B). The data show that Δ133p53-knockdown cells undergo abnormal cell motility in both 2D and 3D cultures, indicating that Δ133p53 is necessary for organized cell movement and development of polarized structures.

We have previously shown that cell–cell adhesion is critical for linking CAMo to acinar morphogenesis and that blocking E-cadherin disrupts CAMo (Tanner et al., 2012). To determine the mechanism underlying the impaired CAMo upon silencing of Δ133p53 isoforms, we measured the expression of E-cadherin in shControl and Δ133p53-knockdown cells grown in 2D and 3D culture (Fig. S5A,B). We observed no significant change between the control and the knockdown cells grown in 2D, whereas E-cadherin expression was slightly increased in Δ133p53-knockdown cells grown in 3D compared with the control. Interestingly, E-cadherin in Δ133p53-knockdown cells cultured in 3D was predominantly localized the center of the 3D structure, whereas control cells displayed a distinct staining pattern at cell–cell adherens junction. These results suggest that Δ133p53-knockdown cells might be loosely adhered, which might partly be responsible for impaired CAMo.

Δ133p53-knockdown cells failed in coherent cell rotation and thus also failed to develop into acinar-like structures, which was accompanied by disruption of apical–basal polarity (Fig. 5C); this is similar to disorganized malignant T4-2 cells. We found that depletion of Δ133p53 in MCF10A cells also causes hollow lumen at the center of acini to fail to form (Fig. 5D), further confirming that Δ133p53 is necessary for formation of polar acinar structure during mammary gland development. Given the results that Δ133p53-knockdown cells displayed an abnormal migratory behavior (Fig. S2A,B), and their CAMo rotation in 3D culture was
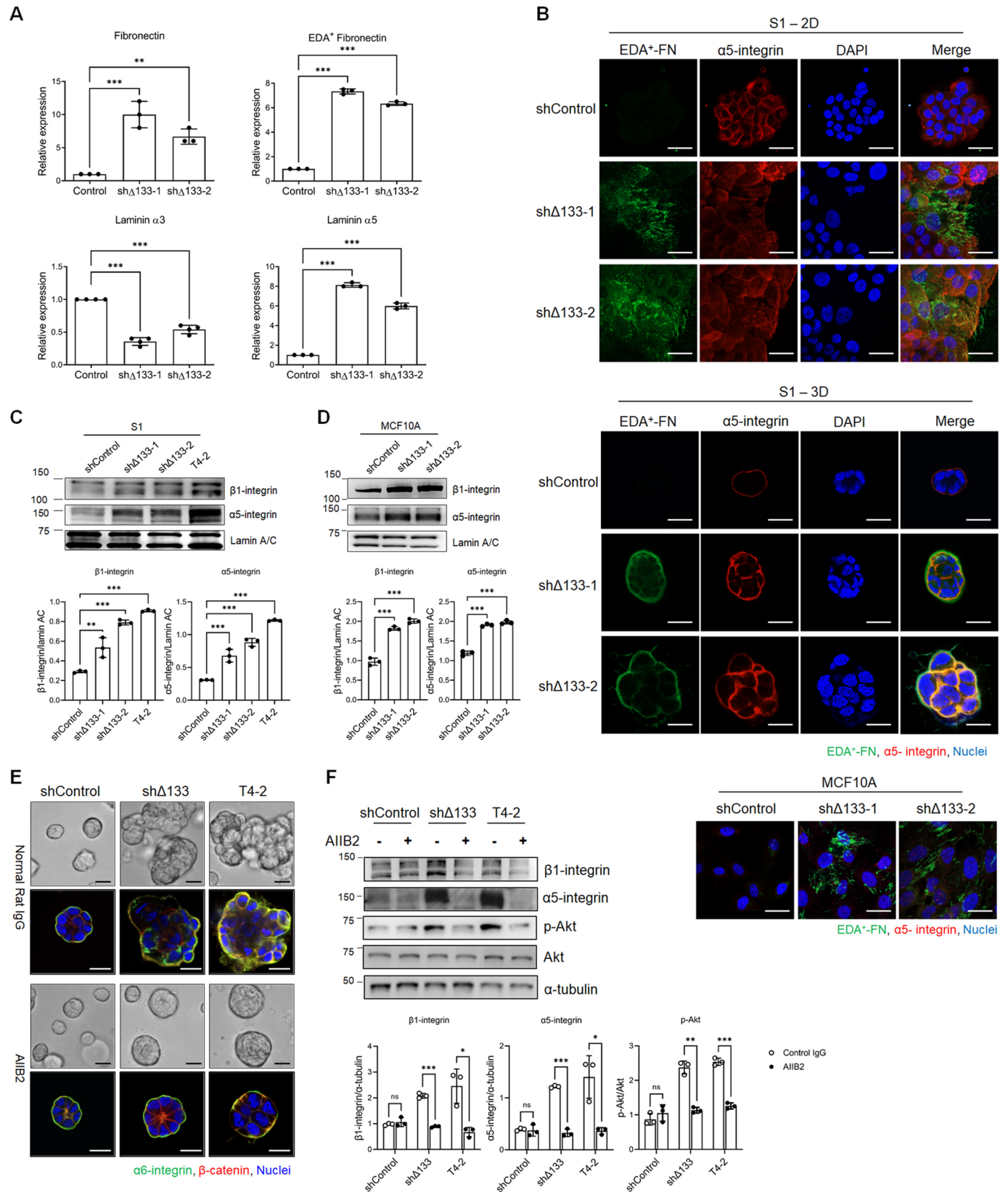
**Fig. 3.** See next page for legend.

**Fig. 3. Δ133p53 isoform coordinates the expression and deposition of fibronectin.** (A) Expression of FN, EDA⁺-FN, and laminin α3 and α5 in control or Δ133p53-knockdown S1 cells grown in 2D was assessed by qPCR analysis. Data are represented as mean±s.e.m. of three independent experiments performed in triplicates and plotted as normalized values with respect to control. (B) Representative confocal images of immunofluorescence staining of EDA-containing fibronectin (green) and α5-integrin (red) in control or Δ133p53 knockdown S1 cells (shΔ133-1 and shΔ133-2) grown in 2D (top) and 3D culture (middle). N=6. Representative images of EDA-containing fibronectin (green) and α5-integrin (red) for shControl and Δ133p53 knockdown MCF10A cells grown in 2D culture (bottom). Nuclei were counterstained with DAPI. N=3. Scale bars: 20 μm. (C) Representative immunoblot and quantification for integrin receptors in control or knockdown S1 grown in 3D. Lamin A/C was used as a loading control. The blots are representative of three independent experiments. (D) Representative immunoblot and quantification for integrin receptors in control or knockdown MCF10A cells grown in 3D. Lamin A/C was used as a loading control. The blots are representative of three independent experiments. (E) Representative images of 3D morphologies of shControl, shΔ133p53 knockdown S1 cells and T4-2 cells treated with either normal rat IgG (150 μg/ml) or AIIB2 (150 μg/ml), an integrin β1 function-blocking antibody. Cells were stained with α6-integrin for a basal polarity marker (green) and β-catenin for a basolateral marker (red). Structure of T4-2 cells was used for comparison. Scale bars: 20 μm. N=4. (F) Representative immunoblot and quantification for α5- and β1-integrin and phosphorylated Akt (p-Akt) in AIIB2-treated shControl, Δ133p53 knockdown S1, and T4-2 cells grown in 3D culture. The level of p-Akt was determined relative to total Akt. T4-2 cells was used for comparison. α-tubulin was used as a loading control. N=3. *P<0.05; **P<0.01; ***P<0.001; n.s., not significant [one-way ANOVA followed by Dunnett's post-hoc test for multiple comparison (A,C,D); unpaired two-tailed Student's t-test (F)].

disrupted and formed disorganized aggregates (Fig. 5C; Movie 4), we therefore conclude that Δ133p53 might dictate proper ECM expression and cytoskeletal movements that are required for CAMo.

## Ectopic expression of Δ133p53 is sufficient to induce polarized acinar formation in malignant cells

Malignant HMT-3522 T4-2 cells carry a mutation on p53 at codon 179 (histidine to glutamine) (Moyret et al., 1994). Given that Δ133p53 was necessary for normal acinar organization, this raised the question of whether the expression of Δ133p53 could compensate for mutant p53. Given that we have observed that the level of Δ133p53 is lower in T4-2 cells than in non-malignant S1 cells (Fig. 1D,E; Fig. S1A,C,D), we investigated whether exogenously expressed Δ133p53 could compensate for mutant p53α and drive T4-2 cells to 'normal' phenotype. T4-2 cells were established using tetracycline-inducible expression system to express an empty vector, or Δ133p53α or Δ133p53β were established using the tetracycline-inducible expression system (Fig. 6A), and their phenotypic changes were analyzed in 3D cultures (Fig. 6B). T4-2 cells expressing Δ133p53 were found to grow into smaller colonies than those with vector-expressing controls, and showed a phenotypically normal acinus-like morphology, including proper polarization of basal and lateral markers (Fig. 6B, bottom; insets). The expression of Δ133p53α or Δ133p53β in T4-2 cells induced downregulation of EDA⁺-FN, α5- and β1-integrin in 3D lrECM (Fig. 6C). In addition, we observed that the cell cycle inhibitor p21 (CDKN1A) as well as phosphorylation of p53 on serine 15 and 46 of p53 were upregulated in Δ133p53α or Δ133p53β expressing T4-2 cells (Fig. 6D). These data confirm that Δ133p53 is necessary and sufficient for establishment and maintenance of polarized breast tissue structure, and can compensate for loss of p53α activity in mutant p53-expressing cells.

## DISCUSSION

Breast epithelial cells discern signals from their surrounding tissue microenvironment and orchestrate gene expression patterns required for mammary gland-specific structure and function. As every cell in a higher organism has the same genetic information, a fundamental problem to solve is how this signal integration occurs and what controls it. Recently, p53 has been found to be one of the critical signaling mediators in morphogenetic pathways (Furuta et al., 2018), and it is becoming evident that canonical full-length p53 and its isoforms have important roles under normal conditions. Although extensive investigation on the cellular and molecular regulation of p53 have revealed its role in protecting cells from tumor progression, our understanding of p53 isoforms remains limited. Here, we investigated the roles of the p53 Δ133p53 isoforms in human breast epithelial cells and found that Δ133p53 modulates the activity of p53 and coordinates mammary gland morphogenesis by regulating the expression of ECM molecules.

We had hypothesized previously that cells interpret information received from their microenvironment and modulate the pattern of gene expression required for establishing and maintaining tissue specificity and homeostasis (Bissell and Hines, 2011). In particular, the interaction between mammary epithelial cells and Ln-1 initiates a signal circuitry and instructs differentiation and the formation of a polarized acinus, the functional unit of mammary gland (Streuli et al., 1995; Furuta et al., 2018). Our current findings show that Δ133p53 expression is increased by Ln-1 exposure (Fig. 1H,I), indicating that Δ133p53 is involved in the signaling pathway that Ln-1 activates for coordinating differentiation and formation of mammary acini (Fig. 7). Our studies support a model whereby, in healthy tissue, Ln-1 induces the expression of Δ133p53 isoforms and in turn these isoforms regulate expression of the crucial laminin subunits LAMA3 and LAMA5, and repress expression of fibronectins (Fig. 7A). However, when Δ133p53 expression is disturbed by dysregulation of splicing events, expression of laminin subunits becomes unbalanced and expression of fibronectins is promoted (Fig. 7B). The increased fibronectins are secreted to the extracellular microenvironment (Fig. 3B) and engage with the α5β1-integrin (Fig. 3E,F), which is known to activate PI3K- or MAPK-associated pathways that promote cell proliferation and survival (Manabe et al., 1999). Changes in fibronectin deposition have been implicated in association with cell migration and invasion (Ruoslahti, 1984). In addition, silencing of Δ133p53 led to an increase in the amount of the laminin α5 chain, which is a component of laminin 511 and 521. Similar to fibronectin, these two laminins also promote cell spreading and migration (Ferletta and Ekblom, 1999). We speculate that excessive deposition of fibronectin surrounding the knockdown cells creates a pro-migratory microenvironment, which results in changes in the migratory behavior of these cells. This creates a positive-feedback loop and leads to actin disorganization, abnormal migratory behavior and apolar structures, which eventually might result in malignant progression. In addition, the time-course pattern of Δ133p53α expression in response to Ln-1 signaling indicates that Δ133p53α expression is regulated in a feed-forward manner (Fig. 1I). Although we did not directly examine the effect of feed-forward regulation by Ln-1, we hypothesize that an altered Ln-1 signaling pathway might lead to an alteration in acinar morphogenesis through perturbed dynamics of Δ133p53 expression, which will be an important area for future study.

We suggest that Δ133p53 could play an important role in the delicate regulation of fibronectin expression, likely in collaboration with p53α. It has been reported that fibronectin promotes
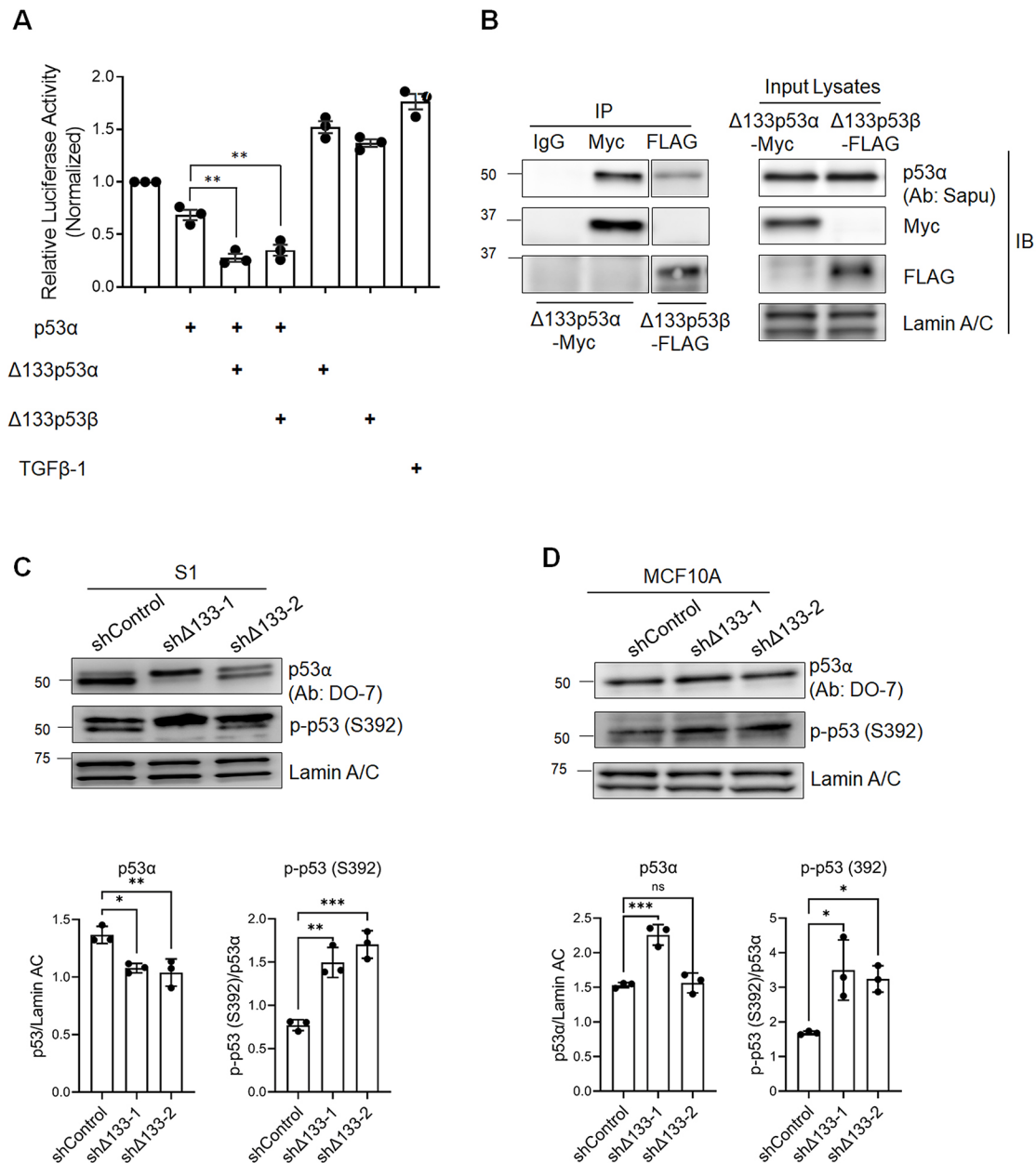
**Fig. 4. Δ133p53 regulates the expression of fibronectin in concert with p53α.** (A) Transcriptional activity of the fibronectin promoter was assessed by a luciferase reporter gene assay in S1 cells. The cells were transfected with pGL3-FN-firefly luciferase and *Renilla* luciferase with a combination of p53α and Δ133p53 isoforms. The active form of the TGFβ-1 vector was used for a positive control. Firefly luciferase activity was correlated for *Renilla* luciferase to normalize the reporter activity. Data are represented as mean±s.e.m. Three independent experiments were performed in triplicate and plotted as normalized values with respect to control vector. (B) Representative results of co-immunoprecipitation (Co-IP) of Δ133p53α or Δ133p53β isoform with an endogenous full-length p53 in 2D culture. S1 cells were transfected with Δ133p53α-Myc or Δ133p53β-FLAG, and the whole lysates were subjected to IP using an antibody against Myc, FLAG, or control IgG, followed by immunoblot analysis with an antibody against full-length p53. *N*=3. (C) Representative immunoblot and quantification for total protein level and phosphorylated level of full-length p53 (p53α) in control or Δ133p53-knockdown S1 cells grown in 3D culture. Lamin A/C was used as a loading control. *N*=3. (D) Representative immunoblot and quantification for total protein level and phosphorylated level of p53α in control or Δ133p53 knockdown MCF10A cells grown in 3D culture. Lamin A/C was used as a loading control. *N*=3. All quantitative results show mean±s.e.m. *$P<0.05$; **$P<0.01$; ***$P<0.001$; n.s., not significant [one-way ANOVA followed by Dunnett's post-hoc test in for multiple comparison (A,C,D)].

organization of collagens into a fibrillar ECM (McDonald et al., 1982). We speculate that enhanced fibronectin produced by the perturbed expression of Δ133p53 might co-assemble into fibrils with collagen, which likely contributes to stiffening of the local extracellular matrix. Consequently, cells assemble actin filaments in response to the stiffness of matrix and modulate their motility and force generation (Zaman et al., 2006). In addition, abnormal localization of E-cadherin exhibited in 3D structure of

Δ133p53-knockdown cells suggests that Δ133p53 influences cell–cell interaction, which requires for proper CAMo. We therefore conclude that Δ133p53 expression is required for appropriate expression of ECM molecules in order to keep ECM in a homeostatic equilibrium and coordinate migratory behaviors. Further study is needed in a 3D context to elucidate whether the dysregulated ECM in Δ133p53-deficient cells directs individual or collective cell migration.
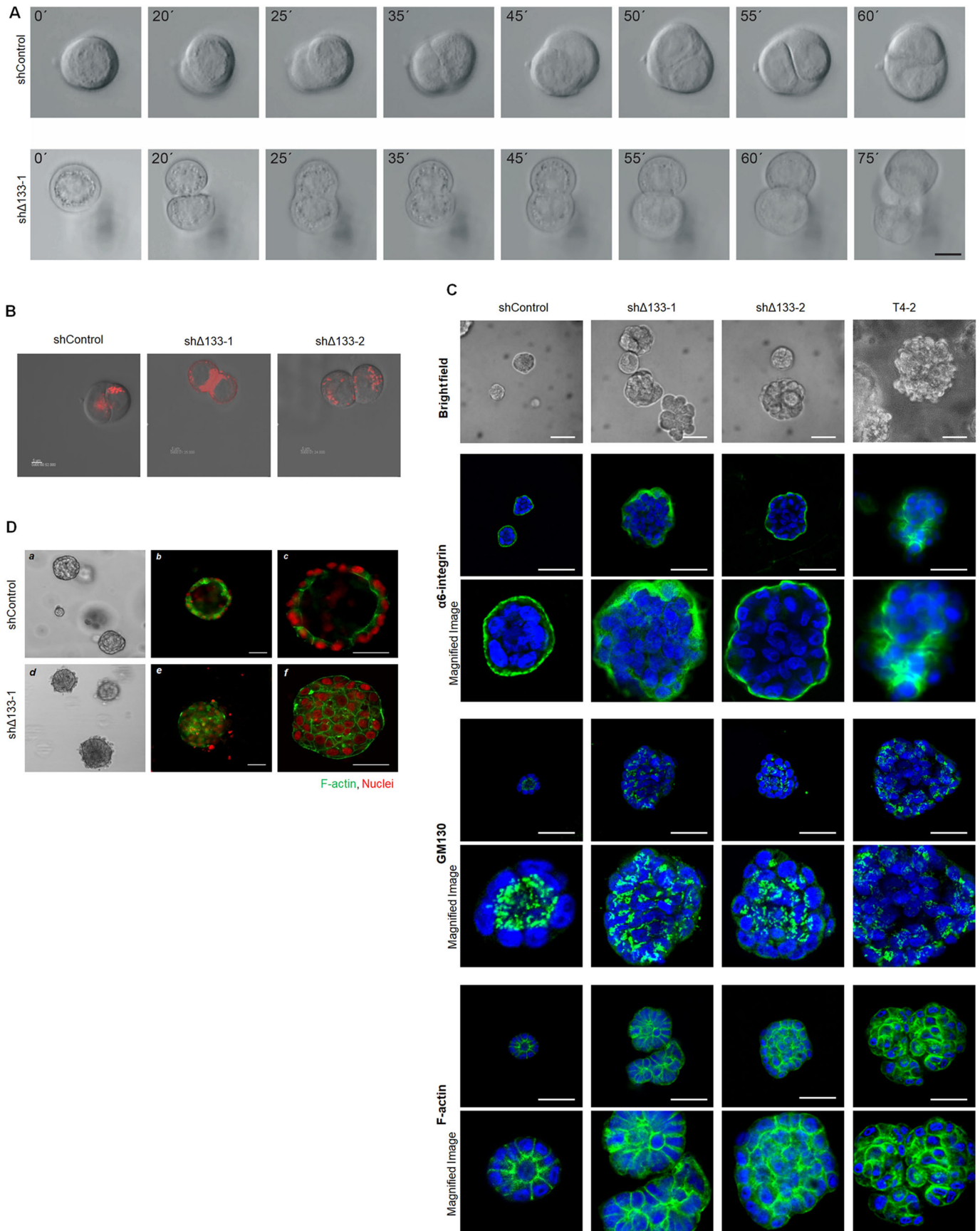
**Fig. 5.** See next page for legend.

**Fig. 5. Δ133p53 is required for establishing and maintaining polar acinar structure.** (A) Representative still images obtained from time-lapse microscopy of control and shΔ133p53 cells in 3D lrECM culture (3D On-Top culture). Scale bar: 7 μm. N=3. (B) Representative still images obtained from time-lapse microscopy of control and shΔ133p53 cells labeled with the lipophilic tracer DiI, in 3D On-Top culture. N=3. Scale bar: 1 μm. (C) Representative phase-contrast and confocal microscope images of α6-integrin, Golgi matrix protein GM130, and F-actin (Alexa 488-Phalloidin) in shRNA control, shRNA Δ133-1, or shRNA Δ133-2 expressing S1 cells grown in 3D On-Top culture. After 10 days of 3D culture, cells were stained with α6-integrin as a basal polarity marker and GM130 as an apical polarity marker. Nuclei were counterstained with DAPI. Structure of T4-2 cells was used for comparison. N=4. Scale bars: 20 μm. (D) Representative phase-contrast (a,d) and immunofluorescence micrographs of control (b,c) or Δ133p53 knockdown (e,f) MCF10A cells in 3D culture. Cells were stained with F-actin (green). Nuclei were counterstained with DAPI. N=3. Scale bars: 20 μm.

The ECM is an essential regulator of tissue-specific form and function (Bruno et al., 2017). Alterations in ECM components, such as increased FN deposition, are associated with tumor progression and the invasive phenotype in cancer (Lu et al., 2012). During mammary gland development ECM undergoes dynamic changes in the composition and structure. Expression of fibronectin is increased during periods of active proliferation, such as the onset of puberty and early pregnancy (Woodward et al., 2001). FN mRNA level is low during pregnancy and lactation, then increased again in involution period (Schedin et al., 2004). 3D culture of MCF10A cells confirmed that fibronectin expression is upregulated in the early proliferative stage of acinar morphogenesis and decreased in the late stages as cells undergo growth arrest (Williams et al., 2008). These findings suggest that tightly controlled ECM expression is critical for normal development and maintenance of tissue structure. However, most transformed cells fail to either synthesize or deposit ECM molecules properly. Our previous study showed that that the expression of EDA$^+$-FN was upregulated in malignant T4-2 cells, as well as its corresponding receptor, α5β1-integrin, compared to levels in non-malignant S1 cells (Nam et al., 2010). Our current data show that T4-2 cells express lower level of Δ133p53 isoforms than S1 cells (Fig. 1D,E) and that silencing of Δ133p53 isoforms in S1 cells leads to an increase of fibronectin expression (Fig. 3A) and a compensatory upregulation of FN-binding α5β1-integrin (Fig. 3C). In addition, our data indicate that recognition of excessively deposited oncofetal EDA$^+$-FN extracellularly by α5β1-integrin might drive cells to promote uncontrolled growth, possibly via the PI3K/Akt pathway (Fig. 3F). We propose that Δ133p53 isoforms exert regulatory influence on expression of proper expression and deposition of ECM molecules, which are critical for normal physiology and homeostasis in mammary epithelial cells.

p53 serves as a transcription regulator that activates or suppresses gene expression in different cellular processes (Riley et al., 2008). Whereas p53 is well known as a transcriptional activator with DNA sequence-specific binding to target gene promoters, there are several reports that p53 represses fibronectin expression by unclear mechanisms (Alexandrova et al., 2000; Iotsova and Stehelin, 1996; You et al., 2017). The p53-mediated repression is presumably achieved by binding to the CCAAT box-binding proteins/factors, namely NF-Y and CBP, which bind to CCAAT sequences on FN promoter (Iotsova and Stehelin, 1996) or by the recruitment of co-repressors, such as histone deacetylase and/or other chromatin-modifying factors (Laptenko and Prives, 2006). Induction of p53 in p53-null immortalized fibroblasts is accompanied by significant cell shape changes and a decrease in FN expression (Alexandrova et al., 2000). In addition, FN expression is significantly decreased by treatment with p53 activator III, RITA, in a breast cancer cell line

(You et al., 2017). These data underscore the significance of p53 in regulation of ECM molecule expression. Indeed, mutant p53 forms a complex with hypoxia-inducible factor (HIF-1) and promotes transcription of type VIIa1 collagen and the laminin-γ2 subunit (Amelio et al., 2018). However, to the best of our knowledge there is no previous report that any p53 isoform is involved in regulation of ECM gene expression. Our results showed that knockdown of Δ133p53 leads to an increase of FN and laminin-α5 expression and a decrease of laminin-α3, coupled with phosphorylation of p53α on serine 392 (Fig. 4C,D). In addition, overexpression of Δ133p53 isoforms in malignant T4-2 cells results in downregulation of FN and phosphorylation of p53α on serine 15 and 46 (Fig. 6D). These findings confirmed that Δ133p53 regulates the expression of ECM molecules by modulating p53α activity. We speculate that Δ133p53 mediates modification of p53α, which in turn accommodates the recruitment and/or interaction of p53α with its binding partners for transcriptional activation or repression of target genes.

Δ133p53 has been shown to modulate p53-induced apoptosis and cell cycle arrest (Bourdon et al., 2005). Evidence for physical interaction between Δ133p53 isoform and full-length p53 has previously been shown in lung cancer cell lines, where Δ133p53 inhibits p53 transcriptional activity on the Bax and p21 promoters (Aoubala et al., 2011). Consistent with this, our current data demonstrate the physical interaction between p53α and Δ133p53 isoforms (Fig. 4B) and cooperative function of the complex in regulation of FN transcription (Fig. 4A). Interestingly, overexpression of Δ133p53 upregulated FN promoter activity in the absence of exogenous p53α, implying that there might be stoichiometric relationships or feedback mechanisms between p53α and Δ133p53 for the regulation of fibronectin expression.

Why do cells need other p53 isoforms if the system has already the canonical p53? A previous study has shown the possibility that the full-length p53 might be regulated by its isoforms (Bourdon et al., 2005). Given the physical interaction of Δ133p53 with p53α and the transcriptional regulation of fibronectin we identified in the current study, our results suggest that Δ133p53 isoform switching serves as one of regulatory mechanisms of p53 signaling; too little or too much of p53 would result in unwanted consequences for ECM homeostasis. p53α and Δ133p53 might have independent roles, but they play cooperative role in fibronectin expression in the developing mammary gland. A recent study has shown that overexpression of Δ133p53 contributes to malignant behavior as well as poor prognosis in breast cancer patients (Gadea et al., 2016). Moreover, increased expression of Δ133p53 isoforms is associated with cell migration and invasion via Jak-STAT3 and RhoA-ROCK signaling pathways (Campbell et al., 2018). Conversely, depletion of Δ133p53 accelerates the onset of senescence in human fibroblast strains (Fujita et al., 2009; von Muhlinen et al., 2018). These previous reports indicate that Δ133p53 might play coordinating roles in a context-dependent manner and that the balanced expression of Δ133p53 is crucial for homeostasis (Joruiz et al., 2020). We speculate that the Δ133p53 isoforms exert pleiotropic functions in a context-dependent manner through stoichiometric binding with its binding partners or cofactors, which potentially confers an increase in regulatory complexity. Therefore, further investigation for cooperativity and stoichiometric relationships among the p53 isoforms is necessary.

A caveat of this study is that the accurate identification of specific p53 isoform by immunoblotting analysis remains ambiguous given that p53 isoforms are detected and identified only by molecular mass.
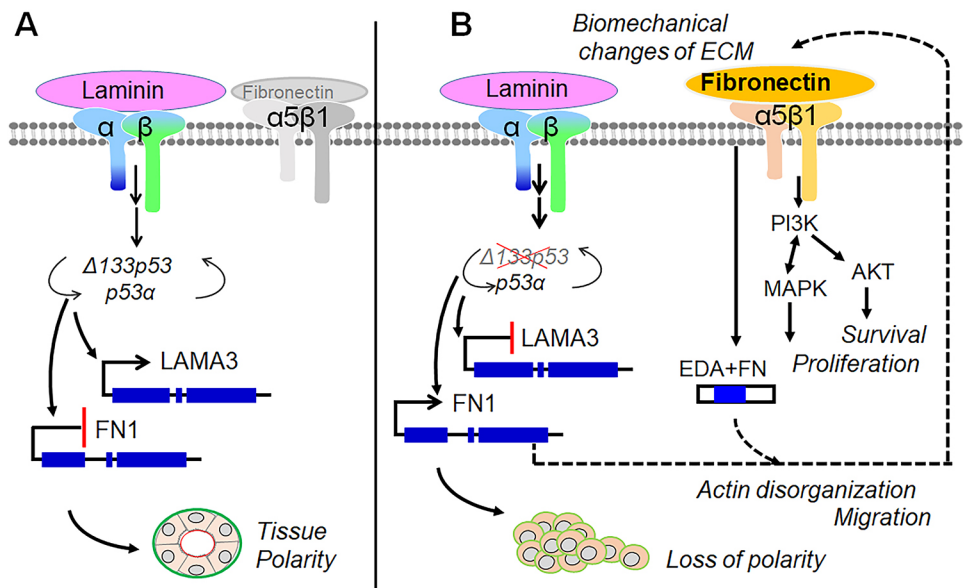
**Fig. 6. Ectopic expression of Δ133p53 is sufficient to induce polarized acinar formation in malignant cells.** (A) Representative immunoblot of Δ133p53α–Myc or Δ133p53β–FLAG isoform expression in T4-2 cells under regulation of doxycycline (Dox). Cells were exposed to Dox at different concentrations for 6 h and subjected to immunoblot analysis using anti-Myc or anti-FLAG antibody. Lamin A/C was used for a loading control. $N$=3. (B) Representative 3D morphology of control, Δ133p53α or Δ133p53β isoform expressing T4-2 cells in the presence of doxycycline. Phase-contrast (top) and immunofluorescence (bottom) stains of α6-integrin as a basal polarity marker (green) and β-catenin (red) as a cell–cell junction marker. Magnified images are shown in the insets. $N$=5. Scale bars: 20 µm. (C) Representative immunoblot and quantification for EDA+-FN, β1-integrin and α5-integrin receptors in control, Δ133p53α or Δ133p53β isoform expression in T4-2 cells cultured in 3D lrECM culture with 1 µg/ml doxycycline. The expression of Δ133p53α and Δ133p53β isoform was confirmed using anti-Myc and anti-FLAG antibodies. α-tubulin was used as a loading control. Four independent experiments performed. (D) The activity of p53 in control, Δ133p53α or Δ133p53β isoform-expressing T4-2 cells cultured in 3D was determined by immunoblot analysis using antibodies specific for phosphorylated p53 (S15, S46 and S392) and p21, a direct transcriptional target of p53. Lamin A/C was used for a loading control. Four independent experiments performed. All quantitative results show mean±s.e.m. *$P<0.05$; **$P<0.01$; ***$P<0.001$; n.s., not significant [one-way ANOVA followed by Dunnett's post-hoc test for multiple comparison (C,D)].

Therefore, careful discrimination among p53 isoforms with very similar molecular mass will be necessary for the future work.

Our studies identify Δ133p53 as an important coordinator for ECM-directed differentiation and morphogenesis of breast acinus. To our knowledge, this study is the first to suggest that Δ133p53 is involved in p53α-mediated regulation of fibronectin gene

expression, a finding that has opened a new avenue of research on the role of p53 in mammary gland development. Moreover, our data indicate that regulation of p53 isoform expression is a previously unexplored dimension in maintenance of form and function in the mammary gland. Further studying the splicing factors in the regulatory networks of p53 isoform switching and their functional

**Fig. 7. Working model for laminin-induced Δ133p53 isoform in acinar morphogenesis.** (A) In healthy tissue, Ln-1 signaling induces the expression of the Δ133p53 isoform. The isoform regulates expression of laminin subunits and fibronectin in concert with p53α, which is required for ECM homeostasis and tissue polarity. (B) The impaired expression of the Δ133p53 isoform leads to changes in laminin subunits and fibronectin expression. Subsequently, extracellular matrix composition is imbalanced and creates a feedback loop, leading to a loss of polarity and an increase of cell proliferation and survival via fibronectin engaged α5β-integrin.

consequences would enable us to identify new pathways that are responsible for progression to malignancy, and in turn might lead to discovery of therapeutic targets for breast and other cancers.

## MATERIALS AND METHODS

### Cell lines and cell culture

HMT-3522 human breast epithelial cell lines consist of non-malignant S1 and malignant T4-2 cells. Non-malignant S1 cells were derived from a tissue of reduction mammoplasty. Malignant T4-2 cells were isolated from mouse tumor formed by injecting pre-malignant cells that were spontaneously established from long-term culture of S1 cells without growth factors. HMT-3522 mammary epithelial cell lines were cultured in a chemically defined H14 medium as previously described (Briand et al., 1987). H-14 medium consists of DMEM/F12 (Thermo Fisher Scientific, #12400-024) with 250 ng/ml insulin (Sigma-Aldrich, I-6634), 10 µg/ml transferrin (Sigma-Aldrich, T-2252), 2.6 ng/ml sodium selenite (BD Bioscience, #354201), $10^{-10}$ M β-estradiol (Sigma-Aldrich, E-2758), $1.4 \times 10^{-6}$ M hydrocortisone (Sigma-Aldrich, H-0888) and 5 µg/ml prolactin (National Institute of Diabetes and Digestive and Kidney Disease). 10 ng/ml epidermal growth factor (EGF; Corning, 354001) was added to H14 medium to culture S1 cells. H14 medium was changed every other day. MCF10A cells were obtained from the American Type Culture Collection (ATCC, CRL-10317), and cultured in DMEM/F12 (Thermo Fisher Scientific, #12400-024) supplemented with 5% horse serum (Hyclone, SH30074), 20 ng/ml EGF (Corning, 354001), 10 µg/ml insulin, 100 µg/ml hydrocortisone, 1 ng/ml cholera toxin (Sigma-Aldrich, C-8052), 50 U/ml penicillin and 50 mg/ml streptomycin. 184D human mammary epithelial cells were a kind gift from Martha Stampfer (Lawrence Berkeley National Laboratory, USA). Cells were periodically tested for mycoplasma contamination with MycoAlert kit (Lonza, LT07-218).

### 3D cell culture

3D On-top culture assay of MCF10A and HMT-3522 cells was performed as described previously (Debnath et al., 2003; Lee et al., 2007). In brief, S1 cells were seeded at 45,000 cells/cm$^2$; and T4-2 cells were plated at 22,500 cells/cm$^2$ on top of pre-coated growth factor-reduced lrECM, a reconstituted basement membrane derived from Engelbreth–Holm–Swarm tumor (Matrigel®; Corning, 354230). After the cells settle on top of lrECM, H14 medium containing 5% Matrigel was added to the plate. The 3D culture of S1 or T4-2 cells was replaced with fresh H14 medium every 2–3 days. For 3D culture of MCF10A cells, cells were seeded at 45,000 cells/cm$^2$ on top of a Matrigel-coated layer and cultured in growth medium (DMEM/F12; Thermo Fisher Scientific) supplemented with 2% horse serum, 5 ng/ml

EGF, 10 µg/ml insulin, 100 µg/ml hydrocortisone, 1 ng/ml cholera toxin, 50 U/ml penicillin, 50 mg/ml streptomycin and 2% Matrigel. The 3D culture was maintained for 15 days and replaced with fresh medium every 4 days. For 3D-Drip culture, cells were initially plated in 2D culture for 18–24 h, and treated with growth medium containing 5% (v/v) lrECM. For reversion of T4-2 cells with AIIB2, cells were incubated with either normal rat IgG (Sigma-Aldrich, I-4131) or AIIB2 (Millipore, MABT409) for 5 min at room temperature and embedded into Matrigel as single cells. For treatment of MAPK inhibitor (PD98959), cells were embedded into Matrigel as single cells and 20 µM of PD98059 or DMSO was added to with growth medium.

### Plasmids

To generate the luciferase reporter, the human fibronectin promoter region from −512 to +268 was amplified from genomic DNA of HMT-3522 S1 cells using primers 5′-CTCGAGTAACAGCTGCAAGGTCGTGG-3′ and 5′-AAGCTTTGAGACGGTGGGGGAGAGAC-3′, and cloned into pGL3-Basic vector (Promega, E1751). To generate Tet-inducible lentviral Δ133p53 expression vectors, C-terminally tagged Δ133p53α (Δ133p53α-MYC) or Δ133p53β (Δ133p53β-FLAG) was cloned into pENTR1A entry vector (Invitrogen, A10462). The following primer sequences were used for the constructs: for Δ133p53α-MYC, 5′-AGATCTCCACCATGTTTTGC-CAACTGGCCAAG-3′ and 5′-GAATTCTCACAGATCCTCTTCTGAGA-TGAGTTTTTGTTCGTCTGAGTCAGGCCCTTCTGT-3′; for Δ133p53β-FLAG, 5′-AGATCTCCACCATGTTTTGCCAACTGGCCAAG and 5′-GAATTCTTACTTGTCGTCATCGTCTTTGTAGTCACAATTTTCTTTT-TGAAAGCTGGTC-3′. pENTR-Δ133p53α-MYC and pENTR-Δ133p53β-FLAG were subsequently inserted into pLenti-CMV/TO-Puro-DEST vector 670-1 (Addgene #17293) that contains Tet Operator sequences (TO) using Gateway LR Clonase (Thermo Fisher Scientific, #11791019) recombination reaction.

### Generation of Tet-inducible cell lines

To establish stable T4-2 cells with Tet-inducible system, T4-2 cells were transfected with the Tet-On vector (Takara Bio, 632104), which expresses reverse tetracycline-controlled transactivator (rtTA) using Fugene 6 transfection reagent (Promega, E2691). Stable clones expressing rtTA were selected with 250 µg/ml G418 (Thermo Fisher Scientific, 10131035) for 2 weeks; then, the stable T4-2 Tet-On cells were infected with lentiviral vector carrying CMV-TO/Δ133p53α-MYC or CMV-TO/Δ133p53β-FLAG. Stable populations of T4-2 cells expressing tet-inducible Δ133p53α-MYC or Δ133p53β-FLAG were selected with 2 µg/ml puromycin (Sigma-Aldrich, P8833). To induce Δ133p53 isoform expression, cells were treated with 1 µg/ml doxycycline (Sigma-Aldrich, D5207).

### Short hairpin RNA

The shRNA systems targeting Δ133p53 isoforms were generated by using RNAi-Ready pSIREN-RetroQ retroviral vector (Clontech, 631526). The oligo pairs were shΔ133-1, 5′-GGAGGTGCTTACACATGTTttcaaga-gaAACATGTGTAAGCACCTCCttttttg-3′ and shΔ133-2, 5′-CTTGT-GCCCTGACTTTCAAttcaagagaTTGAAAGTCAGGGCACAAGttttttg-3′ with lowercase letters representing loop and terminator sequences.

### Virus production

Retrovirus was produced by using Phoenix retrovirus producer cell line. The producer cells were transfected with 2 μg of shRNA plasmid in Opti-MEM (Thermo Fisher Scientific, 31985070) containing a 3:1 (μl:μg) ratio of FuGene6 (Promega)/total plasmid DNA. Retrovirus containing supernatant was harvested 48 h later and filtered through a 0.45 μm syringe filter (Corning). Lentivirus was generated by co-transfection of sub-confluent 293FT cells (Thermo Fisher Scientific, R70007) with pLP1, pLP2, VSVG and transfer plasmid in Opti-MEM containing a 3:1 (μl:μg) ratio of FuGene6/total plasmid DNA. The medium was changed to fresh medium 24 h after transfection, and lentivirus was collected 48 h later and filtered through a 0.45 μm syringe filter.

### Luciferase reporter assay

HMT-3522 S1 cells were co-transfected with pGL3-FN-firefly luciferase reporter plasmid and SV-Renilla luciferase (pRL-SV40; Promega, E2231) in combination of p53α and Δ133p53 isoforms using the Fugene6 transfection reagent (Promega, E2691). The transfection was performed in duplicate with 0.5 μg of pGL3-FN-firefly luciferase reporter vector, 0.05 μg of SV-Renilla luciferase, 0.1 μg of CMV-p53α, and/or SV40-Δ133p53 isoforms. pUC19 plasmid were used for adjusting the DNA concentration for each transfection mixture. Cells were transfected with vector expressing activated TGFβ1 (a gift from A. Roberts, National Cancer Institute, USA) for a positive control. At 24 h after transfection, cells were lysed, and luciferase assay were performed with Dual-Luciferase Assay System (Promega, E1910) according to manufacturer's instruction. Firefly and *Renilla* luciferases were measured by SpectraMax iD3 (Molecular Devices) and firefly reporter activity was normalized with *Renilla* luciferase activity.

### Co-immunoprecipitation and immunoblot analysis

Cells were lysed on ice for 20 min in NP-40 buffer [50 mM Tris-HCl pH 7.4, 250 mM NaCl, 5 mM EDTA, 1 mM NaF, 1 mM Na$_3$VO$_4$, 1% Nonidet 40, and protease and phosphatase inhibitor cocktails (Merck Millipore, 524625)]. The cell lysates were centrifuged for 15 min at 15,800 *g* at 4°C and the supernatant were collected. Concentration of protein lysates was determined using DC protein assay kit (Bio-Rad, 5000111). 500 μg of cell lysate was incubated with 1 μg of antibody coupled with Dynabead (Thermo Fisher Scientific, 10004D) for 4 h at 4°C, and then washed three times with l ml lysis buffer. The beads–protein complexes were incubated for 5 min at 98°C with Laemmli sample buffer. The samples were loaded into 10% or 4-20% Tris-Glycine SDS-PAGE gelss, and transferred to nitrocellulose membrane. After transfer, membranes were blocked in Tris-buffered saline with 0.05% Tween 20 (TBST) with 3% BSA, and subsequently incubated with primary antibody overnight at 4°C. Membranes were then washed with TBST, and incubated with the appropriate HRP-conjugated secondary antibody. Immunoreactive bands were visualized by enhanced chemiluminescent substrate (Pierce) using a Fluorechem 8900 imaging system (Alpha Innotech). Full blot images are shown in Fig. S6.

### Immunofluorescence

Cells were fixed in 4% paraformaldehyde (Electron Microscopy Science, 15710) for 20 min at room temperature. Fixed cells were quenched with phosphate-buffered saline (PBS)/glycine (137 mM NaCl, 10 mM Na$_2$HPO$_4$, 1.8 mM KH$_2$PO$_4$, and 50 mM glycine) and blocked with 10% goat serum (Thermo Fisher Scientific, 16210064) in immunofluorescence buffer (137 mM NaCl, 10 mM Na$_2$HPO$_4$, 1.8 mM KH$_2$PO$_4$, 0.1% BSA, 0.2% Triton X-100, and 0.05% Tween 20). The samples were then incubated with primary antibody overnight at 4°C in a humidified chamber. After intensive rinse in immunofluorescence buffer, Alexa-Fluor-coupled

secondary antibody (Molecular Probes) was incubated with the cells for 1 h at room temperature. Cells were counterstained with DAPI (Sigma-Aldrich, 10236276001) at a final concentration of 0.5 μg/ml. The images were captured and analyzed with a Zeiss LSM 710 confocal microscopy.

### Antibodies and reagents

Primary antibodies used were Sapu (1:3000, Pantropic anti-p53 antibody; Khoury and Bourdon, 2010), KJC12 (1:500, Pantropic anti-p53 antibody), BP53.1 (1:1000, specific for α subclass of p53 isoform; Khoury and Bourdon, 2010), KJC133 (1:1000, specific for Δ133p53, made in-house by J.-C.B.), KJCA160 (1:1000, specific for Δ160p53, made in-house by J.-C.B.), DO-7 (1:2000, Santa Cruz Biotechnology, sc-47698) for recognizing p53α, anti-α-tubulin (1:1000; Santa Cruz Biotechnology, sc-5546), anti-lamin A/C (1:1000; Santa Cruz Biotechnology, sc-20681), anti-β1-integrin (1:1000; BD Biosciences, #610467), anti-α5-integrin (1:1000 for immunoblotting; Santa Cruz Biotechnology, sc-10729), anti-E-cadherin (1:100 for immunofluorescence staining; 1:1000 for immunoblotting; BD Bioscience, #610181), anti-EDA$^+$-FN (1:500 for immunofluorescence staining; 1:1000 for immunoblotting; Abcam, ab6328), anti-GM130 (1:2000; Cell Signaling Technology, #12480), anti-β-catenin (1:50; BD Biosciences, #610154), anti-α5-integrin (1:300 for immunofluorescence staining; Abcam, ab150361), anti-α6-integrin (1:300; BD Biosciences, #555734), anti-Akt (1:1000; Cell Signaling Technology, #9272), anti-phospho-Akt (S473) (1:1000; Cell Signaling Technology, #9271), anti-Myc (1:1000; Thermo Fisher Scientific, PA1-981), anti-FLAG (1:1000; Sigma-Aldrich, F1804), anti-p53 (1:3000; Santa Cruz Biotechnology, sc-47698), anti-phospho-p53 (S9) (1:1000; Cell Signaling Technology, #9288), anti-phospho-p53 (S15) (1:1000; Cell Signaling Technology, #9284), anti-phospho-p53 (S46) (1:1000; Cell Signaling Technology, #2521), anti-acetyl-p53 (K370) (1:1000; Abcam, ab183544), anti-phospho-p53 (S392) (1:1000; Cell Signaling Technology, #9281), Alexa Fluor 488-conjugated Phalloidin (1:1000; Molecular Probes, A12379). Calcein-AM was purchased from Thermo Fisher Scientifics (Invitrogen, C1430). Purified extracellular matrix proteins, namely, fibronectin, collagen IV and collagen I, were from BD Biosciences, and laminin-111 was from Sigma-Aldrich (L-2020).

### Wound healing and cell migration assay

The wound assay for cell migration was performed using Culture-Insert 2 Well (ibidi USA, 80209), which has two cell culture reservoirs separated by a 500 μm wall. In brief, $3\times10^5$ cells were plated in each well of the Culture-Insert 2 Well and incubated at 37°C in a humidified incubator in an atmosphere of 5% CO$_2$ for 48 h. When cells optically reached a 100% confluent layer, the inserts were gently removed and the cell layer was washed with fresh culture medium to remove cell debris and non-attached cells. The monolayer received fresh culture medium, and cell migration was recorded as a time-lapse video for 18 h. Boyden chamber Transwell migration assay was performed with 8 μm Corning® FluoroBlok™ Transwell inserts (Corning, 351152). $10^5$ cells were placed on top the transwell membrane in the upper chamber with complete culture media, and cultured for 48 h. The inserts were transferred into a second 24-well plate containing 4 μg/ml Calcein AM (Thermo Fisher Scientific, C1430) in 1× PBS. The number of cells that migrated to the other side of transwell was quantified by counting the fluorescent cells under a fluorescence microscope (ZEISS Axiovert 2000) at wavelengths of 494/517 nm (Ex/Em).

### Live-cell imaging

Time-lapse images of live cells were acquired with a Zeiss LSM 710 confocal microscope fitted with an environmental chamber to maintain temperature (37°C), humidity and CO$_2$ (5%). shControl-, shΔ133-1- or shΔ133-2-expressing S1 cells were plated in H14 growth medium, and images were acquired every 1 h for 96h.

### qRT-PCR and nested PCR analysis

Total RNA was extracted from cells using RNeasy plus mini kit (Qiagen, 74134), cDNAs were synthesized using Superscript II first strand synthesis kit (Thermo Fisher Scientific, 11904018) and used as templates. Real-time

RT-PCR was performed using LightCycler® 480 SYBR Green I Master (Roche Diagnostics, #04707516001). Primers used for qPCR: α subclass, 5′-AACCACTGGATGGAGAATATTTCAC-3′ and 5′-CAGCTCTGGGA-ACATCTCGAA-3′; β subclass, 5′-AACCACTGGATGGAGAATATTT-CAC-3′ and 5′-TCATAGAACCATTTTCATGCTCTCTT-3′; γ subclass, 5′-AACCACTGGATGGAGAATATTTCAC-3′ and 5′-TCAACTTACGA-CGAGTTTATCAGGAA-3′; Δ133p53, 5′-ACTCTGTCTCCTTCCTCTT-CCTACAG-3′ and 5′-GTGTGGAATCAACCCACAGCT-3′; FN, 5′-CCAAGCTCAAGTGGTCCTGT-3′ and 5′-CACTTCTTGGTGGCCGTA-CT-3′; EDA⁺FN, 5′-CCCTAAAGGACTGGCATTCA-3′ and 5′-GTGG-ACTGGGTTCCAATCAG-3′; LAMA3, 5′-AGCTCTTGCTGAACCG-GATA and 5′-AATGGCTCCCAAAGCTCTCT′; LAMA5, 5′-ACATG-TCCGTCACAGTGGAG-3′ and 5′-TCATTCAGCGTGTCCATCTC′; LAMA1, 5′-AAAGTCGCCGTGTCTGCAGA-3′ and 5′-TTAAAATGAG-TAACCTTCACAGC; TBP, 5′-TGTATCCACAGTGAATCTTGGTTG-3′ and 5′-GGTTCGTGGCTCTCTTATCCTC-3′. For nested RT-PCR, the first reaction was carried out using 5′-GTGTAGACGCCAACTCTCTCTAG-3′ and 5′-GCACACCTATTGCAAGCAAGGGTTC-3′. Primers used for the second reaction were: Δ133p53α, 5′-TAGTGGGTTGCAGGAGGTGCT-3′ and 5′-GTCAGTCTGAGTCAGGCCCTTCTGT-3′; Δ133p53β, 5′-TAG-TGGGTTGCAGGAGGTGCT-3′ and 5′-TTGAAAGCTGGTCTGGTC-CTGA-3′; Δ133p53γ, 5′-TAGTGGGTTGCAGGAGGTGCT-3′ and 5′-CGTAAGTCAAGTAGCATCTGAAG-3′; TBP, 5′-TGTATCCACAGT-GAATCTTGGTTG and 5′-GGTTCGTGGCTCTCTTATCCTC.

## Data analysis on scratch wound images
Migratory fronts on each side were detected by edge detection and cleaned up by morphological operation to detect the front. Then the gap between the two sides was summed to give the area of the scratch at each time point.

## Statistical analysis
Plots include each data points, and all data are expressed as the mean±s.e.m. GraphPad Prism (version 9) Software or MATLAB was used for statistical analysis. Statistical significance was determined by unpaired two-tailed Student's $t$-test, one-way analysis of variance (ANOVA), or two-way ANOVA (with Tukey's, Bonferroni's or Dunnett's post hoc test) as described in the figure legends. A $P<0.05$ was considered statistically significant.

## References
Alcaraz, J., Xu, R., Mori, H., Nelson, C. M., Mroue, R., Spencer, V. A., Brownfield, D., Radisky, D. C., Bustamante, C. and Bissell, M. J. (2008). Laminin and biomimetic extracellular elasticity enhance functional differentiation in mammary epithelia. *EMBO J.* 27, 2829-2838. doi:10.1038/emboj.2008.206

Alexandrova, A., Ivanov, A., Chumakov, P., Kopnin, B. and Vasiliev, J. (2000). Changes in p53 expression in mouse fibroblasts can modify motility and

extracellular matrix organization. *Oncogene* 19, 5826-5830. doi:10.1038/sj.onc. 1203944

Amelio, I., Mancini, M., Petrova, V., Cairns, R. A., Vikhreva, P., Nicolai, S., Marini, A., Antonov, A. A., Le Quesne, J., Baena Acevedo, J. D. et al. (2018). p53 mutants cooperate with HIF-1 in transcriptional regulation of extracellular matrix components to promote tumor progression. *Proc. Natl. Acad. Sci. USA* 115, E10869-E10878. doi:10.1073/pnas.1808314115

Aoubala, M., Murray-Zmijewski, F., Khoury, M. P., Fernandes, K., Perrier, S., Bernard, H., Prats, A.-C., Lane, D. P. and Bourdon, J.-C. (2011). p53 directly transactivates Delta133p53alpha, regulating cell fate outcome in response to DNA damage. *Cell Death Differ.* 18, 248-258. doi:10.1038/cdd.2010.91

Avery-Kiejda, K. A., Morten, B., Wong-Brown, M. W., Mathe, A. and Scott, R. J. (2014). The relative mRNA expression of p53 isoforms in breast cancer is associated with clinical features and outcome. *Carcinogenesis* 35, 586-596. doi:10.1093/carcin/bgt411

Barcellos-Hoff, M. H., Aggeler, J., Ram, T. G. and Bissell, M. J. (1989). Functional differentiation and alveolar morphogenesis of primary mammary cultures on reconstituted basement membrane. *Development* 105, 223-235. doi:10.1242/dev.105.2.223

Berdichevsky, F., Alford, D., D'Souza, B. and Taylor-Papadimitriou, J. (1994). Branching morphogenesis of human mammary epithelial cells in collagen gels. *J. Cell Sci.* 107, 3557-3568. doi:10.1242/jcs.107.12.3557

Bernard, H., Garmy-Susini, B., Ainaoui, N., Van Den Berghe, L., Peurichard, A., Javerzat, S., Bikfalvi, A., Lane, D. P., Bourdon, J. C. and Prats, A.-C. (2013). The p53 isoform, Delta133p53alpha, stimulates angiogenesis and tumour progression. *Oncogene* 32, 2150-2160. doi:10.1038/onc.2012.242

Bernath, V. A., Muro, A. F., Vitullo, A. D., Bley, M. A., Barañao, J. L. and Kornblihtt, A. R. (1990). Cyclic AMP inhibits fibronectin gene expression in a newly developed granulosa cell line by a mechanism that suppresses cAMP-responsive element-dependent transcriptional activation. *J. Biol. Chem.* 265, 18219-18226. doi:10.1016/S0021-9258(17)44741-7

Bissell, M. J. (1981). The differentiated state of normal and malignant cells or how to define a "normal" cell in culture. *Int. Rev. Cytol.* 70, 27-100. doi:10.1016/S0074-7696(08)61130-4

Bissell, M. J. and Hines, W. C. (2011). Why don't we get more cancer? A proposed role of the microenvironment in restraining cancer progression. *Nat. Med.* 17, 320-329. doi:10.1038/nm.2328

Bissell, M. J., Weaver, V. M., Lelievre, S. A., Wang, F., Petersen, O. W. and Schmeichel, K. L. (1999). Tissue structure, nuclear organization, and gene expression in normal and malignant breast. *Cancer Res.* 59, 1757-1763; discussion 1763s-1764s.

Bissell, M. J., Radisky, D. C., Rizki, A., Weaver, V. M. and Petersen, O. W. (2002). The organizing principle: microenvironmental influences in the normal and malignant breast. *Differentiation* 70, 537-546. doi:10.1046/j.1432-0436.2002. 700907.x

Bourdon, J.-C., Fernandes, K., Murray-Zmijewski, F., Liu, G., Diot, A., Xirodimas, D. P., Saville, M. K. and Lane, D. P. (2005). p53 isoforms can regulate p53 transcriptional activity. *Genes Dev.* 19, 2122-2137. doi:10.1101/gad. 1339905

Briand, P., Petersen, O. W. and Van Deurs, B. (1987). A new diploid nontumorigenic human breast epithelial cell line isolated and propagated in chemically defined medium. *In Vitro Cell Dev. Biol.* 23, 181-188. doi:10.1007/BF02623578

Briand, P., Nielsen, K. V., Madsen, M. W. and Petersen, O. W. (1996). Trisomy 7p and malignant transformation of human breast epithelial cells following epidermal growth factor withdrawal. *Cancer Res.* 56, 2039-2044.

Bruno, R. D., Fleming, J. M., George, A. L., Boulanger, C. A., Schedin, P. and Smith, G. H. (2017). Mammary extracellular matrix directs differentiation of testicular and embryonic stem cells to form functional mammary glands in vivo. *Sci. Rep.* 7, 40196. doi:10.1038/srep40196

Campbell, H., Fleming, N., Roth, I., Mehta, S., Wiles, A., Williams, G., Vennin, C., Arsic, N., Parkin, A., Pajic, M. et al. (2018). 133p53 isoform promotes tumour invasion and metastasis via interleukin-6 activation of JAK-STAT and RhoA-ROCK signalling. *Nat. Commun.* 9, 254. doi:10.1038/s41467-017-02408-0

Debnath, J., Muthuswamy, S. K. and Brugge, J. S. (2003). Morphogenesis and oncogenesis of MCF-10A mammary epithelial acini grown in three-dimensional basement membrane cultures. *Methods* 30, 256-268. doi:10.1016/S1046-2023(03)00032-X

Egeblad, M., Rasch, M. G. and Weaver, V. M. (2010). Dynamic interplay between the collagen scaffold and tumor evolution. *Curr. Opin. Cell Biol.* 22, 697-706. doi:10.1016/j.ceb.2010.08.015

Ferletta, M. and Ekblom, P. (1999). Identification of laminin-10/11 as a strong cell adhesive complex for a normal and a malignant human epithelial cell line. *J. Cell Sci.* 112, 1-10. doi:10.1242/jcs.112.1.1

Fiore, A. P. Z. P., Spencer, V. A., Mori, H., Carvalho, H. F., Bissell, M. J. and Bruni-Cardoso, A. (2017). Laminin-111 and the level of nuclear actin regulate epithelial quiescence via Exportin-6. *Cell Rep.* 19, 2102-2115. doi:10.1016/j. celrep.2017.05.050

**Flaman, J. M., Waridel, F., Estreicher, A., Vannier, A., Limacher, J. M., Gilbert, D., Iggo, R. and Frebourg, T.** (1996). The human tumour suppressor gene p53 is alternatively spliced in normal cells. *Oncogene* **12**, 813-818.

**Fletcher, D. A. and Mullins, R. D.** (2010). Cell mechanics and the cytoskeleton. *Nature* **463**, 485-492. doi:10.1038/nature08908

**Freed-Pastor, W. A., Mizuno, H., Zhao, X., Langerød, A., Moon, S.-H., Rodriguez-Barrueco, R., Barsotti, A., Chicas, A., Li, W., Polotskaia, A. et al.** (2012). Mutant p53 disrupts mammary tissue architecture via the mevalonate pathway. *Cell* **148**, 244-258. doi:10.1016/j.cell.2011.12.017

**Fujita, K., Mondal, A. M., Horikawa, I., Nguyen, G. H., Kumamoto, K., Sohn, J. J., Bowman, E. D., Mathe, E. A., Schetter, A. J., Pine, S. R. et al.** (2009). p53 isoforms Delta133p53 and p53beta are endogenous regulators of replicative cellular senescence. *Nat. Cell Biol.* **11**, 1135-1142. doi:10.1038/ncb1928

**Furuta, S., Ren, G., Mao, J.-H. and Bissell, M. J.** (2018). Laminin signals initiate the reciprocal loop that informs breast-specific gene expression and homeostasis by activating NO, p53 and microRNAs. *eLife* **7**, e26148. doi:10.7554/eLife.26148

**Gadea, G., Arsic, N., Fernandes, K., Diot, A., Joruiz, S. M., Abdallah, S., Meuray, V., Vinot, S., Anguille, C., Remenyi, J. et al.** (2016). TP53 drives invasion through expression of its Delta133p53beta variant. *eLife* **5**, e14734. doi:10.7554/eLife.14734

**Gatza, C. E., Dumble, M., Kittrell, F., Edwards, D. G., Dearth, R. K., Lee, A. V., Xu, J., Medina, D. and Donehower, L. A.** (2008). Altered mammary gland development in the p53+/m mouse, a model of accelerated aging. *Dev. Biol.* **313**, 130-141. doi:10.1016/j.ydbio.2007.10.004

**Hall, A.** (1998). Rho GTPases and the actin cytoskeleton. *Science* **279**, 509-514. doi:10.1126/science.279.5350.509

**Hollstein, M., Sidransky, D., Vogelstein, B. and Harris, C. C.** (1991). p53 mutations in human cancers. *Science* **253**, 49-53. doi:10.1126/science.1905840

**Iotsova, V. and Stehelin, D.** (1996). Down-regulation of fibronectin gene expression by the p53 tumor suppressor protein. *Cell Growth Differ.* **7**, 629-634.

**Jarnagin, W. R., Rockey, D. C., Koteliansky, V. E., Wang, S. S. and Bissell, D. M.** (1994). Expression of variant fibronectins in wound healing: cellular source and biological activity of the EIIIA segment in rat hepatic fibrogenesis. *J. Cell Biol.* **127**, 2037-2048. doi:10.1083/jcb.127.6.2037

**Joruiz, S. M., Beck, J. A., Horikawa, I. and Harris, C. C.** (2020). The Δ133p53 isoforms, tuners of the p53 pathway. *Cancers (Basel)* **12**, 3422. doi:10.3390/cancers12113422

**Khoury, M. P. and Bourdon, J.-C.** (2010). The isoforms of the p53 protein. *Cold Spring Harb. Perspect. Biol.* **2**, a000927. doi:10.1101/cshperspect.a000927

**Khoury, M. P. and Bourdon, J.-C.** (2011). p53 isoforms: an intracellular microprocessor? *Genes Cancer* **2**, 453-465. doi:10.1177/1947601911408893

**Laptenko, O. and Prives, C.** (2006). Transcriptional regulation by p53: one protein, many possibilities. *Cell Death Differ.* **13**, 951-961. doi:10.1038/sj.cdd.4401916

**Lee, G. Y., Kenny, P. A., Lee, E. H. and Bissell, M. J.** (2007). Three-dimensional culture models of normal and malignant breast epithelial cells. *Nat. Methods* **4**, 359-365. doi:10.1038/nmeth1015

**Liu, K., Cheng, L., Flesken-Nikitin, A., Huang, L., Nikitin, A. Y. and Pauli, B. U.** (2010). Conditional knockout of fibronectin abrogates mouse mammary gland lobuloalveolar differentiation. *Dev. Biol.* **346**, 11-24. doi:10.1016/j.ydbio.2010.07.001

**Losino, N., Waisman, A., Solari, C., Luzzani, C., Espinosa, D. F., Sassone, A., Muro, A. F., Miriuka, S., Sevlever, G., Barañao, L. et al.** (2013). EDA-containing fibronectin increases proliferation of embryonic stem cells. *PLoS One* **8**, e80681. doi:10.1371/journal.pone.0080681

**Lu, P., Takai, K., Weaver, V. M. and Werb, Z.** (2011). Extracellular matrix degradation and remodeling in development and disease. *Cold Spring Harb. Perspect. Biol.* **3**, a005058. doi:10.1101/cshperspect.a005058

**Lu, P., Weaver, V. M. and Werb, Z.** (2012). The extracellular matrix: a dynamic niche in cancer progression. *J. Cell Biol.* **196**, 395-406. doi:10.1083/jcb.201102147

**Manabe, R., Oh-e, N. and Sekiguchi, K.** (1999). Alternatively spliced EDA segment regulates fibronectin-dependent cell cycle progression and mitogenic signal transduction. *J. Biol. Chem.* **274**, 5919-5924. doi:10.1074/jbc.274.9.5919

**McDonald, J. A., Kelley, D. G. and Broekelmann, T. J.** (1982). Role of fibronectin in collagen deposition: Fab′ to the gelatin-binding domain of fibronectin inhibits both fibronectin and collagen organization in fibroblast extracellular matrix. *J. Cell Biol.* **92**, 485-492. doi:10.1083/jcb.92.2.485

**Moyret, C., Madsen, M. W., Cooke, J., Briand, P. and Theillet, C.** (1994). Gradual selection of a cellular clone presenting a mutation at codon 179 of the p53 gene during establishment of the immortalized human breast epithelial cell line HMT-3522. *Exp. Cell Res.* **215**, 380-385. doi:10.1006/excr.1994.1355

**Nam, J.-M., Onodera, Y., Bissell, M. J. and Park, C. C.** (2010). Breast cancer cells in three-dimensional culture display an enhanced radioresponse after coordinate targeting of integrin α5β1 and fibronectin. *Cancer Res.* **70**, 5238-5248. doi:10.1158/0008-5472.CAN-09-2319

**Nelson, C. M. and Bissell, M. J.** (2006). Of extracellular matrix, scaffolds, and signaling: tissue architecture regulates development, homeostasis, and cancer. *Annu. Rev. Cell Dev. Biol.* **22**, 287-309. doi:10.1146/annurev.cellbio.22.010305.104315

**Pankov, R. and Yamada, K. M.** (2002). Fibronectin at a glance. *J. Cell Sci.* **115**, 3861-3863. doi:10.1242/jcs.00059

**Petersen, O. W., Rønnov-Jessen, L., Howlett, A. R. and Bissell, M. J.** (1992). Interaction with basement membrane serves to rapidly distinguish growth and differentiation pattern of normal and malignant human breast epithelial cells. *Proc. Natl. Acad. Sci. USA* **89**, 9064-9068. doi:10.1073/pnas.89.19.9064

**Riley, T., Sontag, E., Chen, P. and Levine, A.** (2008). Transcriptional control of human p53-regulated genes. *Nat. Rev. Mol. Cell Biol.* **9**, 402-412. doi:10.1038/nrm2395

**Ruoslahti, E.** (1984). Fibronectin in cell adhesion and invasion. *Cancer Metastasis Rev.* **3**, 43-51. doi:10.1007/BF00047692

**Sakai, T., Larsen, M. and Yamada, K. M.** (2003). Fibronectin requirement in branching morphogenesis. *Nature* **423**, 876-881. doi:10.1038/nature01712

**Schedin, P., Mitrenga, T., McDaniel, S. and Kaeck, M.** (2004). Mammary ECM composition and function are altered by reproductive state. *Mol. Carcinog.* **41**, 207-220. doi:10.1002/mc.20058

**Schöck, F. and Perrimon, N.** (2002). Molecular mechanisms of epithelial morphogenesis. *Annu. Rev. Cell Dev. Biol.* **18**, 463-493. doi:10.1146/annurev.cellbio.18.022602.131838

**Seewaldt, V. L., Mrózek, K., Sigle, R., Dietze, E. C., Heine, K., Hockenbery, D. M., Hobbs, K. B. and Caldwell, L. E.** (2001). Suppression of p53 function in normal human mammary epithelial cells increases sensitivity to extracellular matrix-induced apoptosis. *J. Cell Biol.* **155**, 471-486. doi:10.1083/jcb.200011001

**Stampfer, M. R. and Bartley, J. C.** (1985). Induction of transformation and continuous cell lines from normal human mammary epithelial cells after exposure to benzo[a]pyrene. *Proc. Natl. Acad. Sci. USA* **82**, 2394-2398. doi:10.1073/pnas.82.8.2394

**Streuli, C. H. and Bissell, M. J.** (1990). Expression of extracellular matrix components is regulated by substratum. *J. Cell Biol.* **110**, 1405-1415. doi:10.1083/jcb.110.4.1405

**Streuli, C. H., Bailey, N. and Bissell, M. J.** (1991). Control of mammary epithelial differentiation: basement membrane induces tissue-specific gene expression in the absence of cell-cell interaction and morphological polarity. *J. Cell Biol.* **115**, 1383-1395. doi:10.1083/jcb.115.5.1383

**Streuli, C. H., Schmidhauser, C., Bailey, N., Yurchenco, P., Skubitz, A. P., Roskelley, C. and Bissell, M. J.** (1995). Laminin mediates tissue-specific gene expression in mammary epithelia. *J. Cell Biol.* **129**, 591-603. doi:10.1083/jcb.129.3.591

**Tanner, K., Mori, H., Mroue, R., Bruni-Cardoso, A. and Bissell, M. J.** (2012). Coherent angular motion in the establishment of multicellular architecture of glandular tissues. *Proc. Natl. Acad. Sci. USA* **109**, 1973-1978. doi:10.1073/pnas.1119578109

**von Muhlinen, N., Horikawa, I., Alam, F., Isogaya, K., Lissa, D., Vojtesek, B., Lane, D. P. and Harris, C. C.** (2018). p53 isoforms regulate premature aging in human cells. *Oncogene* **37**, 2379-2393. doi:10.1038/s41388-017-0101-3

**Wang, F., Weaver, V. M., Petersen, O. W., Larabell, C. A., Dedhar, S., Briand, P., Lupu, R. and Bissell, M. J.** (1998). Reciprocal interactions between β1-integrin and epidermal growth factor receptor in three-dimensional basement membrane breast cultures: a different perspective in epithelial biology. *Proc. Natl. Acad. Sci. USA* **95**, 14821-14826. doi:10.1073/pnas.95.25.14821

**Weaver, V. M., Petersen, O. W., Wang, F., Larabell, C. A., Briand, P., Damsky, C. and Bissell, M. J.** (1997). Reversion of the malignant phenotype of human breast cells in three-dimensional culture and in vivo by integrin blocking antibodies. *J. Cell Biol.* **137**, 231-245. doi:10.1083/jcb.137.1.231

**Williams, C. M., Engler, A. J., Slone, R. D., Galante, L. L. and Schwarzbauer, J. E.** (2008). Fibronectin expression modulates mammary epithelial cell proliferation during acinar differentiation. *Cancer Res.* **68**, 3185-3192. doi:10.1158/0008-5472.CAN-07-2673

**Woodward, T. L., Mienaltowski, A. S., Modi, R. R., Bennett, J. M. and Haslam, S. Z.** (2001). Fibronectin and the alpha(5)beta(1) integrin are under developmental and ovarian steroid regulation in the normal mouse mammary gland. *Endocrinology* **142**, 3214-3222. doi:10.1210/endo.142.7.8273

**Xu, R., Spencer, V. A. and Bissell, M. J.** (2007). Extracellular matrix-regulated gene expression requires cooperation of SWI/SNF and transcription factors. *J. Biol. Chem.* **282**, 14992-14999. doi:10.1074/jbc.M610316200

**You, D., Jung, S. P., Jeong, Y., Bae, S. Y. and Kim, S.** (2017). Wild-type p53 controls the level of fibronectin expression in breast cancer cells. *Oncol. Rep.* **38**, 2551-2557. doi:10.3892/or.2017.5860

**Zaman, M. H., Trapani, L. M., Sieminski, A. L., Mackellar, D., Gong, H., Kamm, R. D., Wells, A., Lauffenburger, D. A. and Matsudaira, P.** (2006). Migration of tumor cells in 3D matrices is governed by matrix stiffness along with cell-matrix adhesion and proteolysis. *Proc. Natl. Acad. Sci. USA* **103**, 10889-10894. doi:10.1073/pnas.0604460103

**Zhang, Y., Yan, W. and Chen, X.** (2011). Mutant p53 disrupts MCF-10A cell polarity in three-dimensional culture via epithelial-to-mesenchymal transitions. *J. Biol. Chem.* **286**, 16218-16228. doi:10.1074/jbc.M110.214585